NOTE TO USERS

University of Alberta

Studies on self-assembled monolayers and uncrosslinked molecules from polydimethylsiloxane on gold

By

Olutayo Olaseni Ogunwemimo 

A thesis submitted to the Faculty of Graduate Studies and Research in partial fulfillment of the requirements for the degree of Master of Science

Department of Chemistry

Edmonton, Alberta

Fall 2006

Your file Votre référence
ISBN: 978-0-494-22337-6
Our file Notre référence
ISBN: 978-0-494-22337-6

ABSTRACT

Some applications require that the surface of a substrate be chemically modified. Equally important is the characterization of the surface after modification in order to ascertain the success of the process. The research projects presented in this thesis involves the modification of gold substrates with self-assembled monolayers (SAMs) of thiols on the one hand and the study of the diffusion of uncrosslinked molecules of polydimethylsiloxane (PDMS) onto gold substrates.

SAMs of octadecanethiol (ODT) and a mixed SAM of 4-aminothiophenol and ODT on gold were prepared in the conventional way. Cyclic voltammetry and Fourier-transform infrared spectroscopy (FTIR) data obtained confirmed the successful modification of the substrates.

PDMS is the polymer widely used for the patterning of surfaces using micro-contact printing and microfluidic techniques. X-ray photoelectron spectroscopy and FTIR data shows the presence of uncrosslinked PDMS molecules on gold substrates that have had contact with native PDMS.

ACKNOWLEDGEMENTS

"The Lord of Hosts is with us, the God of Jacob is our refuge" Psalm 46:7

I want to thank God for seeing me through this phase of my life. Many times, I felt like giving up, but He always provided a refuge for me.

Dr. J. –B. Green. He is not just my boss, but also a mentor. Thanks so much for all your understanding. I made some mistakes but you always try to put a good construction on everything. You were always there to instruct and advise, not just academically but in other areas of life as well. I do have fond remembrances of you. Thank you so much, I appreciate you.

My wife has been amazing. You have been so full of understanding. Sometimes I come home from campus feeling bad about some experiment that did not work out and you lift me up with gracious words of encouragements. Thanks so much. Little Victoria too has been great, what with those loving and trusting eyes!

My parents and siblings though separated by distance, have nevertheless been overwhelmingly supportive. You are always full of encouragement for me. Good news from your own end also served to inspire me to work harder. My in-laws too have been supportive. I am so very fortunate to have them here with us in Edmonton. Thanks.

Some friends singled out themselves in the way they showed a lot of support and understanding. First are Francis and Comfort Nsiah. Right from my first few days in Edmonton up to the present time, they have been wonderful. Saheed Akonko is indeed a brother, helping with various Microsoft applications and other software. Eli Kenyi helped me to learn how to drive and Olusegun Adebayo was my first 'landlord' in Edmonton, graciously allowing me to stay with him before I got my own accommodation and has been so close to me up until now.

There are other friends and co-workers I cannot forget. In no particular order, they include the Asembias, Toklos, Oresiles, Okeolas, Baiyewuns, Davids, Ndatirwas, Ananas, Sulayman, Khadijat, Martins, Joshua, Olumide, Folarin, Solomon, Shiau-Yin,

Katie, Sandra, Nirala, Derek, Donna, Sherri, Genaro, Rory, Gregory, Dimitre and so many more.

I am grateful to the Faculty of Graduate Studies and Research and the Natural Sciences and Engineering Research Council of Canada (NSERC) for research funding. Thanks also goes to all faculty and support staff of Chemistry department also helped in various ways that only they could have helped, and the whole University of Alberta community for the privilege of studying in this great institution. Thanks to everyone.

Olutayo Ogunwemimo

June 2006

Dedication

Dedicated to my adorable and helpful wife Sudor,
my beautiful daughter Victoria,
and to my loving family in Nigeria and Edmonton.
These all contributed immensely towards my success.

TABLE OF CONTENTS

CHAPTER 1: INTRODUCTION

CHAPTER 2: ATTEMPTED POLYANILINE SINGLE MOLECULE GROWTH USING ELECTROCHEMICAL DIP-PEN NANOLITHOGRAPHY

LIST OF TABLES

LIST OF FIGURES

LIST OF SYMBOLS

h	Planck's constant (6.62×10^{-34} Js)
ν	Frequency (Hz) of radiation
E	Photon energy
cm^{-1}	Wavenumber
Ω cm	Resistivity

LB	Langmuir-Blodgett
lwh	Length width height
MALDI	Matrix Assisted Laser Desorption/Ionization
MCT	Mercury-Cadmium-Telluride detector
mins	Minutes
MOSFET	Metal Oxide Semiconductor Field Effect Transistor
MS	Mass spectroscopy
Ni	Nickel
N_2	Nitrogen gas
ODT	Octadecanethiol
OH	Hydroxyl group
PANI	polyaniline
PDMS	Polydimethylsiloxane
Pd	Paladium
Pt/Ir	Platinum/ Iridium
s	Seconds
SAM	Self-Assembled Monolayers
Si	Silicon
SIMS	Secondary Ion Mass spectroscopy
Str	Stretching vibration
STM	Scanning Tunneling Microscope
Ti	Titanium
TOF	Time of Flight

UV-Vis	Ultraviolet-Visible spectroscopy
V	Volts
W	Tungsten
XPS	X-ray Photoelectron Spectroscopy
μCP	Microcontact printing
μm	Microns
^{1}H NMR	Proton Nuclear magnetic resonance spectroscopy
4-ATP	4-aminothiophenol

CHAPTER 1

INTRODUCTION

There is quite a lot of research that is focused on tailoring the surface properties of substrates for various applications. In order to ascertain the successful tailoring of the surface properties, a detailed characterization of the modified surfaces is necessary. The characterization methods will determine the structure, composition and distribution of the molecules on the surface. There are many techniques available for surface characterization, which include microscopy-based methods and spectroscopy based methods.

1.1 Microscopy based methods.

Atomic Force Microscopy (AFM) [1] generally involves the use of a small probe scanned across the substrate surface to obtain information about the surface. Such information includes topography [2] or other physical [3], chemical [4] or magnetic [5] properties of a surface. The probe has a very sharp tip, often less than 30nm in diameter, attached to the end of a small cantilever beam. The probe is mounted on a piezoelectric scanner tube, which then scans the tip across the sample surface. The tip-sample interaction causes the cantilever to deflect as the surface properties changes. A laser beam focused on the back of the cantilever is reflected, onto photodiode array detectors. Feedback mechanisms enable the piezoelectric scanners to maintain the tip at a constant force (height information) or constant height (force information) above the sample surface.

AFM can work in several modes among which are contact and tapping modes. In contact mode, the tip scans the sample in close contact. When there are changes in surface topography for example, the cantilever deflects and the scanner adjusts the tip position in order to restore the original cantilever deflection (constant force). There could be sample damage however, due to the close contact of the probe to the surface. In tapping mode [6], the probe intermittently comes in contact with the surface and then lifts up to avoid dragging the tip across the surface thereby avoiding sample damage. The tip has sufficient oscillation amplitude to overcome tip-sample adhesion, which results as the sample intermittently touches the surface. When the tip passes over a

bump on a surface, the cantilever's oscillation amplitude is decreased, and conversely when the tip passes over a depression on a surface, the oscillation amplitude is increased. The system monitors the tip position and oscillation amplitude in order to identify and measure surface features.

AFM is also used for many other applications such as dip-pen nanolithography where the tip is used to transfer patterns onto substrate surface, and in electrochemical dip-pen nanolithography in which the probe is used to carry out localized reactions on a substrate surface. These two would be dealt with in detail later on.

Scanning Tunneling Microscopy (STM) [7] is based on the flowing of tunneling current when an atomically sharp metallic tip and a conductive substrate are in very close proximity. When a voltage is applied between the metallic tip and the conductive substrate, a tunneling current will flow. The direction of the current depends on the polarity of the voltage. If the sample is biased negative relative to the tip, electrons will flow from the sample surface to the tip, and vice versa. The current is exponentially related to the tip-sample separation and directly proportional to the applied voltage. As with the AFM, there are two modes of operation of the STM: constant height mode (current data recorded) and constant current mode (height data recorded). The basic mode however, is the constant current mode in which the tip height is adjusted as the tip is moved across the surface in order to keep the current constant.

1.2 Spectroscopy based methods.

Two important spectroscopies for surface characterization are Fourier transform infrared spectroscopy (FTIR) and x-ray photoelectron spectroscopy (XPS). The technique of FTIR involves the measurement of the absorption (or transmission) of infrared radiation by the sample. The molecules absorb the frequencies of radiation that matches the vibrations which creates a net change in the dipole moment of the molecule. The wavelengths that are absorbed are characteristic of the molecular structure. Excited molecules can undergo two types of molecular vibrations i.e. stretching vibration and bending vibration. In a stretching vibration, there is a change in inter-atomic distance along the bond axis, which may be either symmetric or asymmetric while in bending vibration, there is change in angle between two bonds.

Bending vibrations includes rocking, scissoring, wagging and twisting. Figure 1.1 shows some of these vibrations.

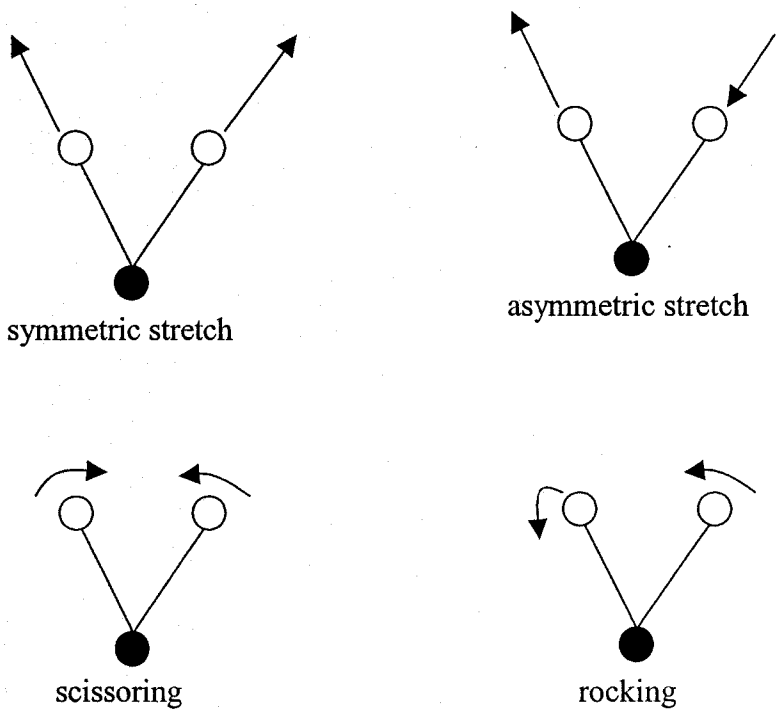

Figure 1.1 shows some of the vibration modes that excited molecules undergoes. The stretching vibrations are higher energy vibrations compared with bending vibrations.

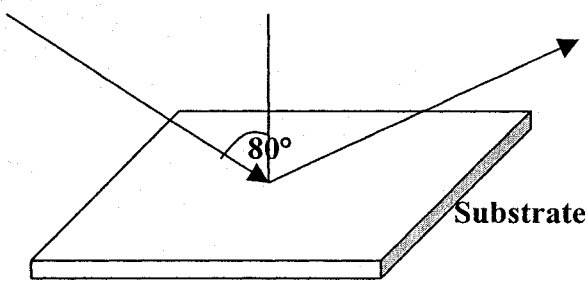

Figure 1.2 is a schematic of FT IRRAS technique. Infrared light interacts with the sample at grazing angle and the reflected light is measured by the detector.

The mode of FTIR used in the studies presented in this thesis is the Infrared reflection-absorption spectroscopy or IRRAS. The technique makes use of polarized incident light at high incident angles. This enhances the absorption of infrared radiation by thin films of molecules on highly reflective surfaces such as gold. IR beam can be resolved into the so-called p and s components of radiation where p is the parallel-polarized radiation and s is the perpendicular polarized radiation. The electric field amplitude of the p-polarized light peaks around the grazing angle while that of the s-polarized is negligible at all angles. Thus surface species can give signals after absorption of p-polarized light at grazing angle of incidence. The spectra obtained are peaks representing specific functional groups.

In XPS, a material is irradiated with monochromatic x-rays, the atoms absorb the photons, which leads to the ionization of core electrons. Depending upon the binding energy of the electrons they will be ejected with different kinetic energies (KE) as expressed by this equation $KE = h\nu - \Delta E$

The ΔE is referred to as the binding energy of the electron. The number of photoelectrons emitted as a function of their kinetic energy (or binding energy) is measured to give rise to a spectrum. Therefore, each element will have characteristic binding energies for each inner core atomic orbital. The peak areas can be used with appropriate sensitivity factors to determine the composition of the surface. The shape of each peak and the biding energy can be affected by the chemical environment of each atom, so chemical bonding data can also be inferred. Figure 1.3 is a simple schematic of the XPS process.

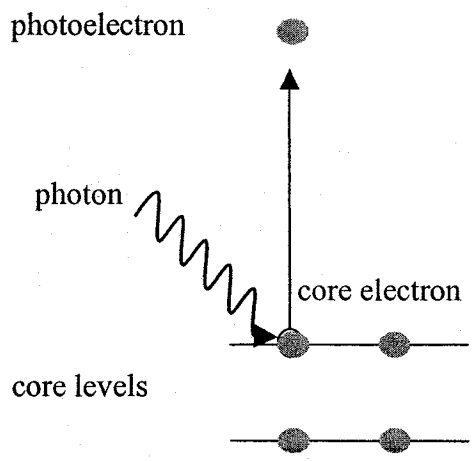

Figure 1.3 is a simple schematic of the XPS process. The x-ray photon is absorbed by an atom in a sample, which then leads to the removal of the core electrons. The number of electrons emitted (intensity) are then measured and recorded as a function of the kinetic energy to yield a spectrum.

1.3 The need for single molecule electronics

The basic subunit of electronic computers is the transistor, which is built upon crystalline, doped Si (the pure form of Si is a poor conductor). Over the past four decades or so, the size of the transistor has been reduced tremendously to nanometer size in order to function effectively in ultradensely integrated electronic circuits and faster processors. The smaller sizes will eventually become more difficult and expensive to fabricate. Photolithography is currently used to make integrated circuits.

A type of transistor known as Field Effect Transistor (FET) is made up of a polysilicon gate electrode, and source and drain channels. The FETs work by controlling the migration of electrons or holes into conduction channel between a source and drain electrode when a voltage is applied between the gate and source. This polysilicon gate has an ultra-thin layer of SiO_2 which acts as an insulator (resistivity in excess of 10^{16} Ωcm) separating the gate from the semiconductor. It is now possible to produce FETs and integrated circuits with gate oxides less than 10 atoms across. A study by Muller *et al* [8] however, showed that the electrical insulation of the gate oxide breaks down with only four atomic layers in the SiO_2. Clearly then, there is a limit to the scaling down process and other suitable alternative sources might be necessary.

As far back as the mid 70's, Ratner and Aviram [9] suggested, using some semi-quantitative calculations, that molecules could be used as components in active electronic devices. Molecular electronics involves replacing the transistor and other basic solid-state electronic elements with one or few molecules. One good point is the fact that molecules are nanometer scale structures, and so are much smaller in area than the current semiconductor silicon-based devices. For measurement of current-voltage (I-V) characteristics of these molecules, STM and conducting AFM are ideal tools. In STM, the molecules are assembled on a conductive substrate and probed with an atomically sharp metallic tip. For conducting AFM, conductive probes are used.

1.4 Are single molecules conductive?

A single molecule is a chain of molecules composed of repeating units bound together by conjugated π- bonds to allow mobile electron flow. The electronic properties of these single molecules are dependent on the degree of π-delocalization.

With conjugation, the electrons are more de-localized compared with non-conjugated molecules where there is less electronic communication between one end of the molecule and another. One obvious question is whether these single molecules are actually conductive. An ideal molecular wire should be able to transfer charge over long distances and at a fast rate.

Several experiments have investigated the conductivity of "single molecules". Using crossed wire junctions, a sandwich of metal-molecule-metal was used to record I-V measurements [10, 11]. Tour and co-workers also performed conductance measurements on self assembled monolayers of benzene-1,4-dithiol on Au using mechanically controllable break junctions [12]. Stoll *et al* [13] used an STM tip to image individual molecules of copper phthalocyanine adsorbed on polycrystalline silver surfaces under ultra-high vacuum conditions. Bumm *et al* [14. 15] used an STM tip to measure the conductivity of single molecules embedded in a self-assembled monolayer of dodecanethiolate. An electromechanical amplifier was demonstrated using a single fullerene (C60) molecule by applying a small force in the nano-Newton range with the aid of an STM tip [16]. Dekker *et al* [17] used electrostatic trapping to deposit a single nanoparticle of Pd between two metal electrodes and then measured the electron transport.

For the design of molecules for unimolecular devices, decision on assemblage must be made. For the assemblage, physisorption and chemisorption are two methods that could be used. Physisorption involves the physical adsorption of molecules onto a solid substrate, for example, Langmuir-Blodgett monolayer. Chemisorption involves the self-assembly of molecules on substrates such as gold or oxidized silicon by covalent bond formation of end groups such as thiols and chlorosilanes respectively.

1.5 Langmuir-Blodgett monolayers

Langmuir film consists of amphiphilic molecules spread on a liquid surface like water. Langmuir-Blodgett (LB) films are prepared by transferring Langmuir films onto a solid substrate. For molecular electronics applications, the LB films can be useful for creating extremely thin layer of organic molecules of uniform thickness. The suitable molecule must be such that one end is able to strongly interact with water (hydrophilic head group) while the other end (hydrophobic end group) must be hydrophobic enough

that the whole molecule cannot dissolve in water. A monolayer of loosely packed molecules is formed first on the water surface, which can be made more compact by reducing the area of the water surface. The uniform monolayer is then deposited on a substrate [18, 19]. Repeating the deposition step many times forms multilayers of the molecules. There have been some proposals for the applications of LB films for passivating the surface of photoconductive devices [20], as a gate insulator in field effect transistor [21], and ultrasonic transducer [22]

1.6 Self-Assembled Monolayers (SAMs)

Self-assembled monolayers are ordered molecular assemblies formed by the spontaneous adsorption of the molecules from solution or the gas phase onto the surface of solid substrates to form crystalline or semicrystalline structures. The adsorbed SAM molecules are used to modify the interfacial properties of metals, semiconductors and other substrates. The molecules that form SAMs have specific chemical functionalities, or 'headgroup', which usually have a high affinity for the substrate surface. Various headgroups in literature demonstrates specific affinity for different substrates. A schematic of a SAM is shown in Figure 1.4. The most common ones are alkanethiols on Au [23, 24, 25], Ag [26, 27, 28]. SAMs are easily prepared and do not require specialized equipments as is the case for LB monolayers. The SAMs of alkanethiols on gold usually have low density of defects, are stable under ambient laboratory conditions and are useful as ultrathin resists for fabrication of structures.

Various types of substrates have been used for SAMs; the more common are thin metal films on glass, Si or mica, single crystals, nanorods, nanocrystals etc. One of the ways by which these substrates can be prepared is by physical vapor deposition using a thin adhesion layer of Ti or Cr, and then the metal of interest. Electrolesss deposition using chemical reduction of metal salts is another method of preparing the substrates. Before the use of the substrates, cleaning treatments have to be applied such as the use of "piranha" solution (solution of 3:1 concentrated H_2SO_4 and 30% H_2O_2) and ultraviolet ozone cleaning. Even though SAMs can be packed to high densities to form high quality electron and ion-transfer barriers, defects and pinholes are still possible due to a number of reasons, which may include, but are not limited to, factors

such as the cleanliness of the substrate and the purity of the solution of the molecules forming the SAMs.

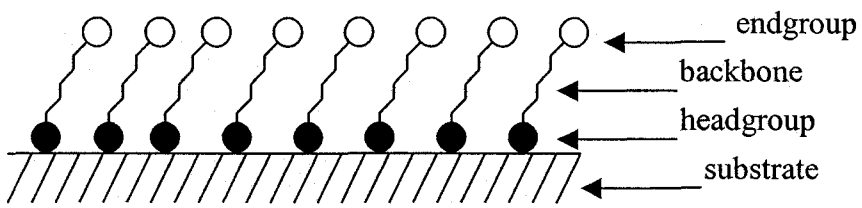

Figure 1.4: A schematic of a self-assembled monolayer showing the headgroup (e.g. thiols) and the endgroup (e.g. OH, COOH). The backbone is made up of methylene chains.

1.6.1 Mixed SAMs

This comprises of mixture of molecular structures. Two driving forces for mixed SAMs are the tailoring of surface energy and wetting properties by mixing different components, and the need for chemical patterning of surfaces. Co-adsorption of the different thiols from solution using various mole fractions has been reported for preparing mixed SAMs of thiols. Earlier works showed that there was phase separation of the co-adsorbed molecules to some extent, that is, the components of the SAMs were not randomly dispersed on the surface but similar molecules appeared to aggregate together into small "islands" [29, 30]. Another study however showed, using infrared spectroscopy (IR) that there are no intermolecular interactions between neighboring hydroxyl (OH) groups in HS-$(CH_2)_{16}$-OH, thus indicating random mixing rather than single component island formation [31]. Some other studies have supported the case for phase separation rather than random mixing [32], using STM [33] and AFM [34].

1.6.2 Preparation of SAMs

SAMs of organosulfur compounds form spontaneously on gold substrates either from solution or via the vapor phase.

1.6.2.1 Preparation from solution:

The solvent most commonly used for preparing SAMs of alkanethiols is ethanol which is able to solvate many of these SAM molecules having varying polarity and chain lengths. Other solvents such as tetrahydrofuran, acetonitrile, toluene [35] also formed SAMs that were not significantly different from those formed from ethanol though some studies suggest that the kinetics for the formation of SAMs in solvents such as hexanes and heptanes is faster than in ethanol [36, 37]. The overall formation kinetics depends on the relative solubility of the alkanethiol in the solvent.

In order to prepare a SAM from solution, there is immersion of a clean substrate into a 1-10mM ethanolic solution of thiols for 12-18 hours at room temperature. A proper rinsing procedure has to be followed to rid the substrate of unbound molecules. Dense coverages are obtained from such dilute solutions within a few minutes. Then a slow reorganization process begins that involves conformational changes of the

molecules with each other, with the substrate and with the solvent in order to minimize any defects in the SAM, which may take hours. Studies have shown that the average properties of thiol SAMs (such as wettability) do not change significantly when immersed in 1mM solutions for more than 18 hours but the coverage increases with extended immersion times which means the number of defects in the SAM decreases. Some applications may require such longer period of immersion [38].

1.6.2.2 Adsorption from gas phase

One method that has been applied successfully makes use of an ultra high vacuum chamber, which allows for substrate cleaning, by say, ion sputtering, and the subsequent deposition by gas phase [39, 40]. Chemisorption of thiols onto gold using nitrogen purge stream containing the necessary vapor has also been reported. [41]

1.6.2.3 Scanning probe lithography

Mirkin and co workers [42, 43] demonstrated the use of an AFM tip to write alkanethiols on a gold film with a resolution down to 5nm. The AFM tip is likened to a "dip-pen" while the molecules to be transferred onto a substrate are referred to as the "inks". The "inking" process can be achieved by dipping the AFM tip into a solution of interest. The molecules from the tip are then directly deposited onto the substrate. This is referred to as dip-pen nanolithography (DPN). Figure 1.5 is a schematic of the DPN process. The mechanism for the transport of molecules from the AFM tip onto the substrate is not clearly understood yet. There is still some debate as to what role, if any, water plays in the transport process [44, 45]. This process depends on some variables such as humidity, tip velocity and temperature [46].

Other application of scanning probe lithography includes writing hexamethyldisilazane (HMDS) ink on semiconductor Si/SiO_x and oxidized GaAs surfaces [47]. The tip of a scanning probe microscope can also be used to scratch a surface [48] where a layer of photoresist on a substrate was burrowed through with the tip of an AFM to form desired patterns and the resist subsequently etched to reveal the desired pattern on the substrate. Anodic oxidation of Si [49-52] has also been demonstrated by applying a negative bias to the tip in order to oxidize the underlying Si or H-passivated substrates.

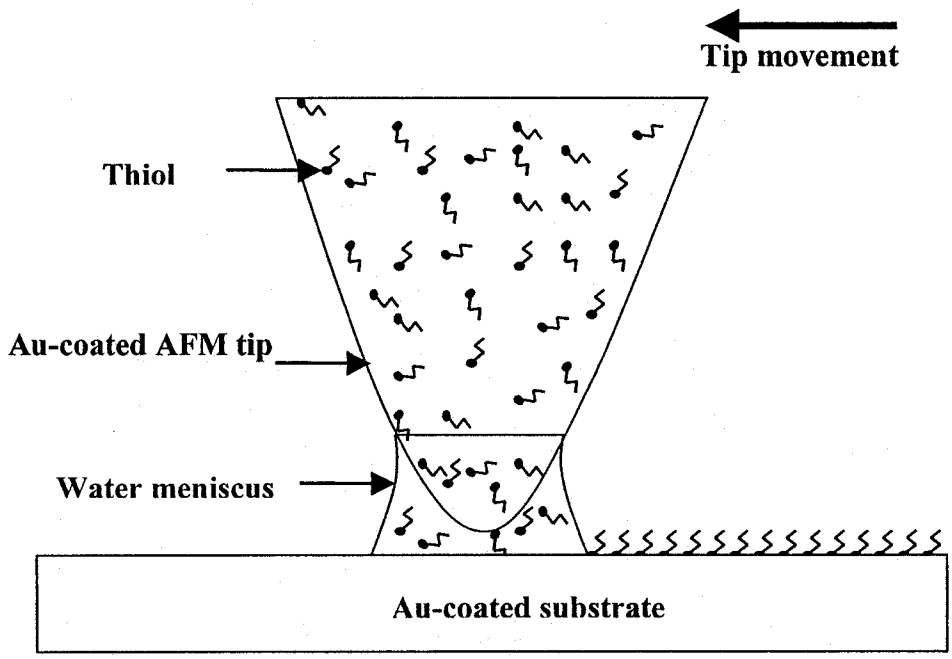

Figure 1.5: Schematic of the DPN process. The tip is coated with the desired molecule to be transferred, dried and brought into contact with the substrate. The patterns made follow the tip movement.

1.6.2.4 Soft Lithography

In soft lithography [53], an elastomeric stamp is used to transfer patterns to a substrate. Soft lithography encompasses techniques, which includes microcontact printing [54], replica molding [55], microtransfer molding [56], micromolding in capillaries [57], solvent-assisted micromolding [58] and microfluidics

1.6.2.4.1 Microcontact printing (μCP)

Elastomeric patterning methods, such as micro-contact printing (μCP) and microfluidics are used to create two-dimensional structures on a surface. μCP involves the use of an elastomeric stamp with the desired relief features, which is then 'inked' with the SAM molecule of interest, dried and brought into conformal contact with a substrate. Only the regions that are exposed to the stamp are modified with the SAM. Figure 1.6 shows the steps involved in μCP. Polydimethylsiloxane or PDMS is the elastomer most commonly used for many applications. The side of the PDMS facing the Si wafer during the curing process is used for printing. However, the time required to form SAM from solution is relatively longer than that from micro-contact printing and it is a dry process. One study actually suggests that the quality of SAM of alkanethiol using μCP is different from that assembled from solution [59].

μCP has many problems however, such as 1) swelling of the PDMS during inking; 2) hydrophobicity of the PDMS; 3) stamp deformation and 4) transfer of PDMS molecules onto the substrate. Swelling of the PDMS during the inking process might result in patterns with increased size, thus affecting the resolution of the patterns on the substrate as excess ink molecules diffuse across the surface [60]. Hydrophobicity of the PDMS used to be a problem with polar inks, but surface modification by processes such as oxygen plasma and corona discharge can create hydrophilic surfaces. The use of a moderately hydrophilic stamp that is based on poly(ether-ester) co-polymer [61] provides another alternative solution to this problem. Stamp deformation leads to distortion of the patterns on the surface [62]. Suh *et al* [63] developed a deformation-proof stamp to help combat the problem.

Perhaps the biggest problem is the contamination of the substrate by uncrosslinked PDMS molecules. There have been quite a number of reports on this

issue [64-69]. Ways of getting rid of this contamination effects includes the use of organic solvents such as heptane [70] and hexane [71] to extract the uncrosslinked PDMS molecules, and ultraviolet/ozone [72] modification to the polymer.

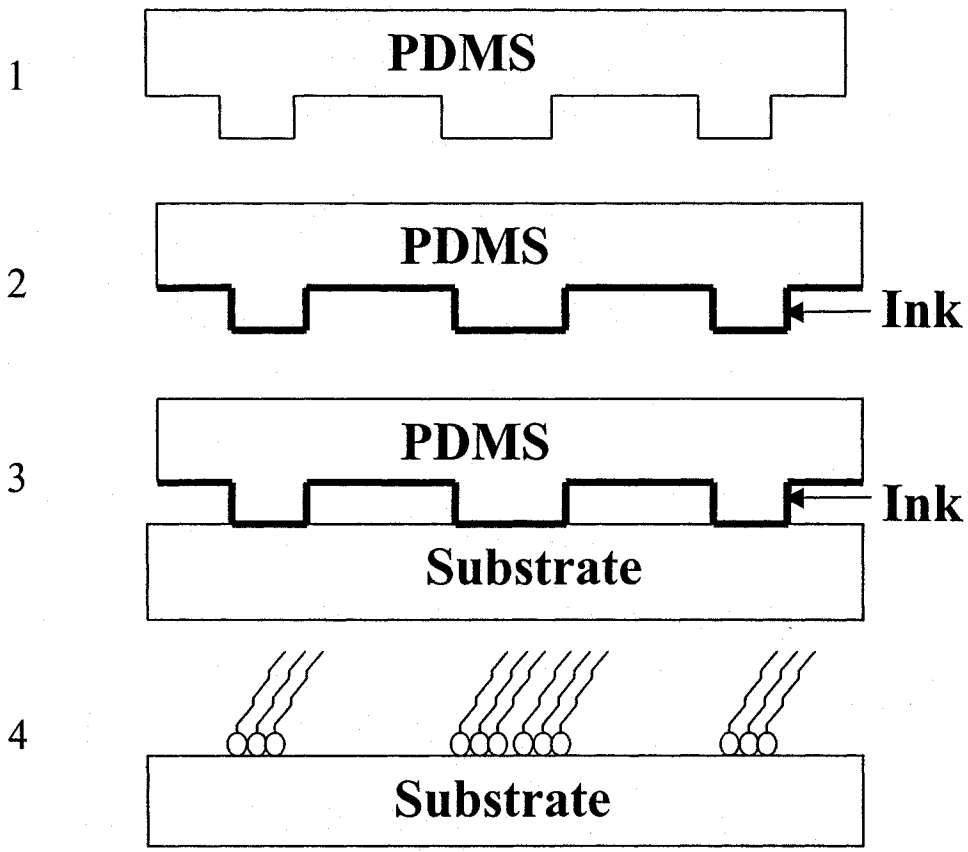

Figure 1.6 is a schematic of the microcontact printing process. The PDMS elastomer (1) is inked with the desired molecules to be patterned and dried (2). The inked stamp is then brought into conformal contact with the substrate (3). After being in contact for the desired length of time, the PDMS is removed from the surface leaving a pattern of the ink molecules in regions where there was contact with the substrate.

μCP has been used to pattern different kinds of molecules on various substrates, for example, alkanethiols on gold [73, 74], proteins on glass [75, 76], and polymers on reactive SAMs [77, 78], to mention just a few. We used μCP in the study of the contaminants from polydimethylsiloxane. The only difference was there was no ink used.

1.6.2.4.2 Microfluidic based patterning.

Microfluidics involves the manipulation of liquids in channels of miniaturized systems having cross-sectional dimensions approximately 10-100μm as seen in Figure 1.7. Small volumes of samples and reagents are used in microfluidic networks to localize reactions on or pattern substrates. Microfluidic systems have been used to pattern cells and proteins on substrates [79, 80]. Most of the earlier works were done in microfluidic networks fabricated in silicon and glass [81-83], but silicon is a relatively more expensive material compared with PDMS, and relatively more time-consuming and expensive to fabricate devices in silicon and glass than in PDMS. Microfluidic networks in PDMS are easy to fabricate, fast and cheap, but there is also the possibility of contamination from the PDMS molecules.

1.6.3 Characterization of SAMs

Many methods are has been reported in literature as tools for the characterization of SAMs. The more common ones that have been used include spectroscopic methods such as infrared spectroscopy [84, 85], ellipsometry [86] and X-ray photoelectron spectroscopy [87]. Methods based on scanning probe microscopies have also been used to provide direct image of the structure: AFM [88] and STM [89]. The different methods provide different information with the target being the understanding of the whole picture. While spectroscopic methods generally average over macroscopic lengths (which means they detect molecules in ordered and possibly disordered areas) and are often sensitive to the tilt angle of the molecular backbone, AFM would provide topographic and other required data.

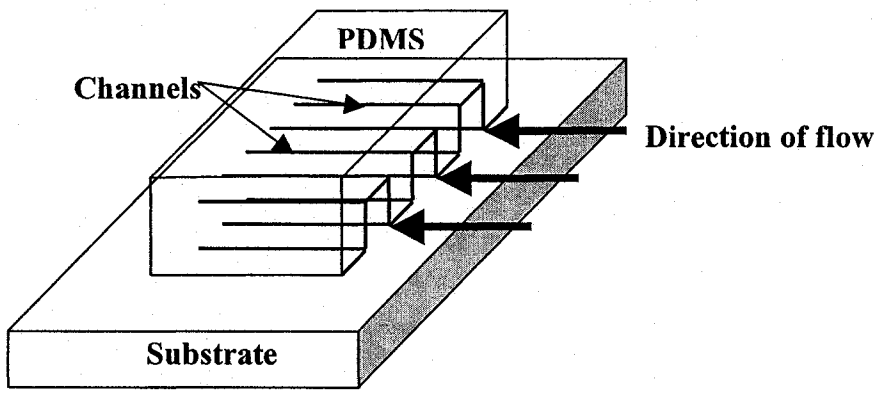

Figure 1.7 shows a schematic of a typical microfluidic network used for patterning surfaces. The channels are made inside the PDMS with cross channels on the order of 10-100 μm. After patterning, the PDMS is easily removed.

1.7 Polydimethylsiloxane (PDMS)

PDMS comprises of repeating units of O-Si-$(CH_3)_2$- with a Si-O backbone. The CH_3 groups make the surface of the PDMS hydrophobic. PDMS is a very compliant elastomer such that conformal contact with the substrate can be achieved. PDMS can cure at low temperatures, can be deformed reversibly and is non-toxic, so cell cultures can be grown on it. High hydrophobicity, contamination resistance, and long-term endurance and durability make PDMS a very useful polymer for insulation, anticorrosion, and antifouling coatings. The elastic characteristic of PDMS also allows it to be released easily from masters during fabrication and from substrates. PDMS has low surface and bulk conductivity to prevent any electrical current from flowing through the bulk material, and high fracture toughness over a wide temperature range. PDMS provides a surface that is low in interfacial free energy, chemically inert, optically transparent down to about 300 nm and so can be used with a number of detection systems, for example, UV-Vis absorbance and flourescence. The surface properties of PDMS can be readily modified by treatment with plasma [90].

Most of the PDMS stamps used in literature were fabricated from Sylgard-184, which is a commercially available two-component kit manufactured by Dow Corning. The first is made up of a base consisting of dimethylsiloxane oligomers with vinyl terminated end groups, Pt catalyst, and silicone filler and the second component is the curing agent containing a crosslinking agent (dimethyl methylhydrogen siloxane) and an inhibitor (tetramethyl tetravinyl cyclotetrasiloxane). PDMS is usually prepared using replica molding by casting the liquid prepolymer of an elastomer against a master that has a patterned relief structure in its surface. In most applications, the fabricated PDMS was used without any further modification while in other cases the surface of the PDMS has to be modified to make it more hydrophilic. The increased hydrophilicity enables the printing of hydrophilic molecules by micro contact printing.

1.8 Polymerization methods for conducting polymers.

Generally conducting polymers (CPs) can be synthesized by a wide range of methods, principally electrochemically and by chemical oxidation.

1.8.1 Electrochemical Polymerization

Electrochemical polymerization [91, 92] is carried out by adopting a standard three-electrode cell configuration in a supporting electrolyte potentiometrically (to obtain thin films using constant potential) or galvanometrically (for thick films using constant current). The monomers are oxidized to get polymers in their oxidized, doped state. To get the neutral polymer, the oxidized polymer must be reduced, either electrochemically or chemically.

1.8.2 Chemical Polymerization

Chemical polymerization is carried out without any electrodes. The monomers are first oxidized to a cation radical with the help of an oxidizing agent such as $FeCl_3$. These cation radicals then couple repeatedly to form the polymer [93, 94].

1.8.3 Template Synthesis

Template synthesis involves the use of nanoporous membranes, which serves as templates for the electrochemical [95], or chemical oxidation [96, 97] polymerization of monomers. For the electrochemical pathway, a surface of the membrane is coated with a metal film, which then serves as the anode while in the chemical template synthesis pathway; the membrane is simply immersed in a solution containing both the desired monomer and the oxidizing agent. The CPs produced this way have been shown to have enhanced conductivity of about an order of magnitude compared with bulk samples [98, 99]

1.8.4 Electrochemical Dip-pen Nanolithography

This is very similar to DPN: a water meniscus is formed between the tip and the substrate that contains the molecules to be transferred. This water meniscus is used to transport the ink molecules. In E-DPN however, the water meniscus is used as a tiny electrochemical cell and a positive or negative bias is applied to the AFM tip to drive electrochemical reactions within the nanometer-sized meniscus, as shown in Figure 1.8. The tip is moved across the surface in a preprogrammed way [100-102].

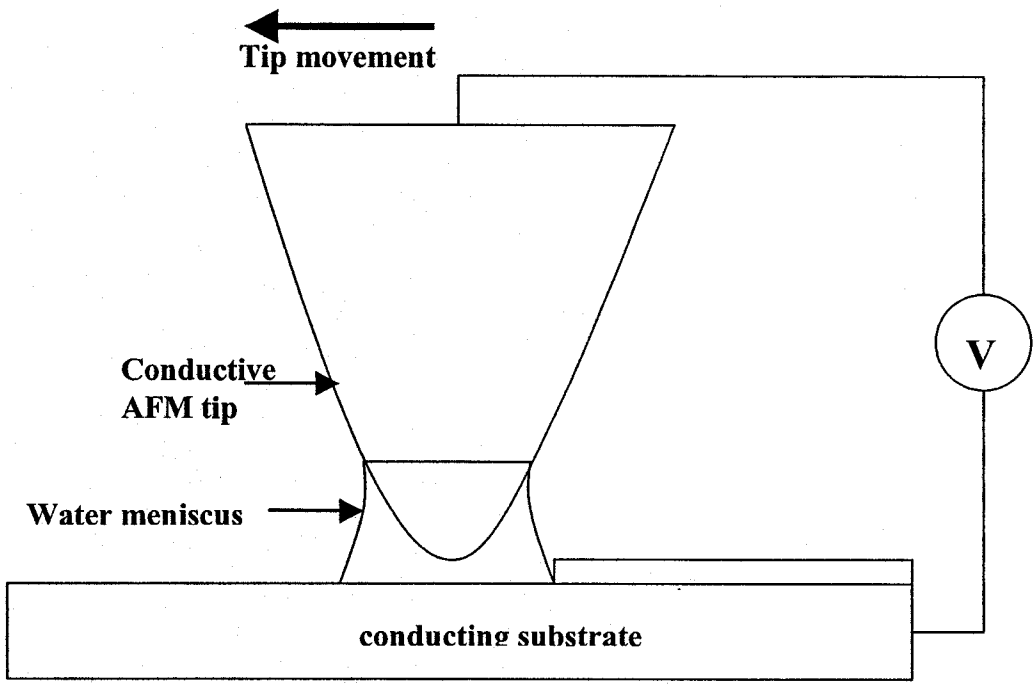

Figure 1.8 shows a schematic for electrochemical dip-pen nanolithographic set-up. The tip is coated with the desired 'ink' and bias applied to the tip while keeping the substrate at ground potential.

E-DPN has been used to pattern peptide/proteins onto Ni surface by applying a negative bias to the tip and keeping the substrate at ground potential [103]. Liu J. *et al* [104] demonstrated the writing (fabrication) of Pt metal on a doped Si surface by applying a positive bias to the tip to cause reduction of the metal salt.

1.9 Research objectives:

The original idea was to use electrochemical dip pen nanolithography to polymerize aniline from the gas phase on a mixed monolayer of ODT and 4-ATP. In order to do this, it was important to understand the cyclic voltammetric behavior of aniline on ODT, 4-ATP and on mixed monolayers of ODT and 4-ATP. There was also the need to characterize the monolayers formed using FT IRRAS.

1.10 References:

1. G. Binnig, C. F. Quate, C. Gerber, *Phys. Rev. Let.* **1986,** *56*, 930.
2. M. M. Maye, I. I. S. Lim, J. Luo, Z. Rab, D. Rabinovich, T. B. Liu, C. J. Zhong, *J. Am. Chem. Soc.* **2005**, *127*, 1519.
3. W. Q. Shi, Z. Q. Wang, S. X. Cui, X. Zhang, Z. S. Bo. *Macromolecules* **2005**, *38*, 861.
4. S. S. Tan, R. L. Sherman, D. Q. Qin, W. T. Ford, *Langmuir* **2005**, *21*, 43.
5. D. Morecroft, J. L. Prieto and M. G. Blamire *J. Appl. Phys.* **2005**, *97*, 10C518
6. Q. Zhong, D. Inniss, K. Kjoller, V. B. Elings, *Surf. Sci.* **1993**, *290*, L688.
7. R.M. Feenstra *Surf. Sci.* **1994**, *299/300*, 965-979
8. D.A. Muller, *Nature,* **1999,** *399,* 758-761
9. A. Aviram, and M. Ratner, *Chemical physics letters,* **1974**, *29*, 277-283
10. J.M., Tour, *Chemical European Journal*, **2001**, *7(23)*
11. J. G. Kushmerick, D.B. Holt, J.C. Yang, R. Shashidhar, J. Naciri, M.H. Moore *Phys. Rev. Lett.* **2002**, *89*, 086802-1 -086802-4
12. M. A. Reed, C. Zhou, C. J. Muller, T. P. Burgin, J. M. Tour, *Science*, **1997,** *252*, 278
13. J.K. Gimzewski, E. Stoll and R.R. Schlittler, *Surface Science,* **1987,** *181,* 267-277
14. M. T. Cygan, T. D. Dunbar, J. J. Arnold, L. A. Bumm, N. F. Shedlock, T. P. Burgin, L. Jones, D. L. Allara, J. M. Tour, P. S. Weiss, *J. Am. Chem. Soc.* **1998**, *120*, 2721.
15. L. A. Bumm, J. J. Arnold, M. T. Cygan, T. D. Dunbar, T. P. Burgin, L. Jones, D. L. Allara, J. M. Tour, P. S. Weiss, *Science* **1996**, *271*, 1705
16. C. Joachim, J.K. Gimzewski, *Chemical Physics Letters,* **1997,** *265*, 353-357
17. A. Bezryadina C. Dekker and G. Schmid *Applied Physics Letters,* **1997,** *71*
18. B. Mann and H. Kuhn *Journal Applied Physics* **1971**, *42* , 4398
19. H. Kuhn *Thin Solid films,* **1983**, *99*, 1
20. K. K. Kan, G. G. Roberts and M. C. Petty *Thin Solid Films,* **1983,** *99,* 291- 296
21. J. P. Lloyd, M. C. Petty, G. G. Roberts, P. G. Lecomber and W. E. Spear *Thin Solid Films.* **1983,** *99,* 297-304
22. J. R. Drabble, and S. M. Al-Khowaildi, *Thin Solid Films,* **1983,** *99,* 271-275
23. C. D. Bain, J. Evall, and G. M. Whitesides *J. Am. Chem. Soc.* **1989**, *111,* 7155-7164

24. M. D. Porter, T. B. Bright, D. L. Allara, and C. C. *J. Am. Chem. Soc.* **1987,** *109,* 3559

25. P. E. Laibinis,G. M. Whitesides, D. L. Allara,Y.-T. Tao, A. N. Parikh, and R. G. Nuzzo *J. Am. Chem. Soc.* **1991**, *113,* 7152

26. G. M. Whitesides, D. Qin, J. Tien, and Y. Xia, *Langmuir* **1996,** *12,* 4033

27. M. M. Walczak, C. Chung, S. M. Stole, C. A. Widrig, and M. D. Porter *J. Am. Chem.*

Soc. **1991**, *113,* 2310

28. P. Fenter and P. Eisenberger, J. Li, N. Camillone, S. Bernasek, G. Scoles, T. A. Ramanarayanan and K. S. Liang *Langmuir* **1991**, 7, 2013-2016

29. J. P. Folkers, P. E. Laibinis, and G. M. Whitesides *Langmuir* **1992**, *8*, 1330-1341

30. J. P. Folkers, P. E. Laibinis, and G. M. Whitesides *J. Phys. Chem.* **1994**, *98,* 563-571

31. L. Bertilsson and B. Liedberg *Langmuir* **1993**, *9,* 141-149

32. S. V. Atre, B. Liedberg, and D. L. Allara *Langmuir* **1995**,*11,* 3882-3893

33. S. J. Stranick, A. N. Parikh, Y.-T. Tao, D. L. Allara, and P. *S.* Weiss *J. Phys. Chem.* **1994**, *98*, 7636-7646

34. K. Tamada, M. Hara, H. Sasabe, and W. Knoll *Langmuir* **1997**, *13,* 1558-1566

35. D. Colin, G. M. Whitesides, and R. *G.* Nuzzo *J. Am. Chem. Soc.* **1989**, *111,* 321-335

36. O. Dannenberger, J. J. Wolff, and M. Buck *Langmuir* **1998,** *14,* 4679-4682

37. K. A. Peterlinz and R. Georgiadis *Langmuir* **1996,** *12,* 4731-4740

38. C. E. D. Chidsey *Science (Washington, D.C.)* **1991**, *251*, 919

39. P. Schwartz , F. Schreiber, P. Eisenberger and G. Scoles *Surface Science* **1999,** *423* 208–224

40. G. E. Poirier *Langmuir* **1999,** *15,* 1167-1175

41. R. C. Thomas, Li Sun, and R. M. Crooks *Langmuir* **1991**, *7*, 620-622

42. R. D. Piner, J. Zhu, F. Xu, S. Hong, C. A. Mirkin *Science* **1999,** *283*, 661

43. S. Hong, J. Zhu, C. A. Mirkin *Science 286*, 523

44. P. V. Schwartz, *Langmuir* **2002**, *18*, 4041

45. R. D. Piner, J. Zhu, F. Xu, S. H. Hong, C. A. Mirkin, *Science* **1999**, *283*, 661.

46. S. Rozhok, R. Piner, C. A. Mirkin, *J. Phys. Chem. B* **2003**, *107*, 751

47. C. A, Mirkin, A. Ivanisevic *J.Am. Chem. Soc* **2001**, *123(32)*, 7887

48. U. Kunze and B. Klehn *Adv. Mater.* **1999**, *11(17)*

49. B. Legrand and D. Stievenard *Appl. Phys. Lett.*, **1999**, *74(26)*

50. P. Avouris, R. Martel, T.Hertel, R. Sandstrom *Appl. Phys. A* **1998**, *66*, S659–S667

51. Y. Matsuzaki, K.-I. Yuasa, J. Shirakashi, E. K. Chilla, A. Yamada, M. Konagai *Journal of Crystal Growth* **1999**, *201/202*, 656-659

52 J.A. Dagata, J. Schneir, H.H. Harary, C.J. Evans, M.T. Postek, J. Bennett, *Appl. Phys.*

Lett. **1990**, *56*, 2001

53 R. S. Kane, S. Takayama, E. Ostuni, D. E. Ingber and G. M. Whitesides *Biomaterials*

1999, *20*, 2363-2376

54 A. Kumar and G. M. Whitesides, *Applied Physics Letters*. **1993**, *63*, 2002

55. Y. Xia, E. Kim, X.-M. Zhao, J. A. Rogers, M. Prentiss, G. M. Whitesides, *Science* **1996**, 273, 347-349.

56. X.-M. Zhao, S. P. Smith, S. J. Waldman, G. M. Whitesides, M. Prentiss, *Appl. Phys. Lett.* **1997**, *71*, 1017-1019.

57. Y. Xia, E. Kim, G. M. Whitesides, *Chem. Mater.* **1996**, *8*, 1558-1567.

58. E. Kim, Y. Xia, X.-M. Zhao, G. M. Whitesides, *Adv. Mater.* **1997**, *9*, 651-654.

59. I. Bohm, A. Lampert, M. Buck, F. Eisert, M. Grunze, *Appl. Surf. Sci* **1999**, *141*. 242

60. A. P. Quist, E. Pavlovic, S. Oscarsson, *Anal. Bioanal. Chem* **2005**, *381,* 591-600

61. D. C. Trimbach, M. Al-Hussein, W. H. de Jeu, M. Decre, D. J. Broer, and C. W. M. Bastiaansen *Langmuir* **2004**, *20,* 4738-4742

62. J. A. Rogers, K. E. Paul, and G. M. Whitesides *J. Vac. Sci. Tech. B* **1998**, *16*, 88-97

63. K. Y. Suh, R. Langer and Lahann *J Appl. Phys. Lett.* **2003**, *83*, 4250-4252

64. K. Pandian and G. A. Nirmala *J Solid State Electrochem* **2003**, *7* 298

65. M. L. Tingey, S. Wilyana, E. J. Snodgrass, and N. L. Abbott *Langmuir* **2004**, *20* 6823

66. K. Felmet and Y.-L. Loo *Appl. Phys. Lett.*, **2004**. *85*, 3317

67. J. Rickert, T. Weiss, W. Gtpel *Sensors and Actuators B* **1996** *31,* 45-50

68. C. J. Powell, A. Jablonski, W. S. M. Werner and W. Smekal. *Appl. Surf. Sci* **2005,** *239,* 470.

69 W. Prissanaroon, N. Brack, P.J. Pigram, P. Hale, P. Kappen, J. Liesegang *Thin Solid Films*, **2005**, *477,* 131

70. A. Kumar, H. A. Biebuyck, G.M. Whitesides *Langmuir* **1994,** *10*, 1498-1511

71. D. J. Graham, D. D. Price and B. D. Ratner *Langmuir* **2002** *18,* 1526

72. K. Glassmaster, J. Gold, A. Andersson, D.S. Sutherland and B. Kasemo, *Langmuir*, **2003**, *19*, 5475

73. E. Delamarche, H. Schmid, A. Bietsch, N. B. Larsen, H. Rothuizen, B. Michel, and H. Biebuyck *J. Phys. Chem. B* **1998**, *102,* 3324-3334

74. A. Kumar, H. A. Biebuyck, and G. M. Whitesides *Langmuir* **1994**, *10,* 1498-1511

75. J. P. Renault, A. Bernard, A. Bietsch, B. Michel, H. R. Bosshard, and E. Delamarche

J. Phys. Chem. B **2003**, *107,* 703-711

76. A. Bernard, E. Delamarche, H. Schmid, B. Michel, H. R. Bosshard and H. Biebuyck *Langmuir,* **1998,** *14(9),* 2225

77. L. Yan, W. T. S. Huck, X.-M. Zhao, and G. M. Whitesides *Langmuir* **1999**, *15,* 1208-

1214

78. J. Lahiri, E. Ostuni, and G. M. Whitesides *Langmuir* **1999**, *15,* 2055-2060

79. E. Delamarche, A. Bernard, H. Schmid, A. Bietsch, B. Michel, H. Biebuyck, *J. Am. Chem. Soc.* **1998**, *120*, 500-508

80. E. Delamarche, A. Bernard, H. Schmid, B. Michel, H. Biebuyck, *Science* **1997**, 276, 779-781

81. A. Manz, D. J. Harrison, K. Seiler, *Anal. Chem.* **1993**, *65,* 1481-1488

82. N. Chiem, D. J. Harrison, *Anal. Chem.* **1997**, *69*, 373-378

83. J.P. Kutter, S. C. Jacobson, N. Matsubara, J. M Ramsey. *Anal. Chem.* **1998**, *70*, 3291-

3297

84. R. G. Nuzzo, L. H. Dubois, and D. L. Allara *J. Am. Chem.* Soc., **1990,** *112, (2), 559*

85. A. N. Parikh and D. L. Allara *J. Chem. Phys.* **1992,** 96 (2),

86. C. D. Bain, E. B. Throughton, Y.-T. Tao, J. Evall,G. M.Whitesides, R. G. Nuzzo, *J. Am. Chem. Soc.* **1989**, *111*, 321-335.

87. J. P. Folkers, P. E. Laibinis, G. M. Whitesides, *Langmuir* **1992**, *8*, 1330-1341

88. C. A. Alves, E. L. Smith, M. D. Porter, *J. Am. Chem. Soc.* **1992**, *114*, 1222-1227

89. C. A. Widrig, C. A. Alves, and M. D. Porter *J. Am. Chem.* Soc., **1991**, *113,(8),* , 2805

90. K. Efimenko, W. E. Wallace, and J. Genzer *J. of Col. and Interface Science,* **2002**, *254*, 306

91. W. A. Hayes, C. Shannon, *Langmuir* **1996**, *12*, 3688.

92. R. J. Willicut, R. L, McCarley,. *J. Am. Chem. Soc.* **1994**, *116*, 10823

93. S. A. Chen and C. -C. Tsai *Macromolecules* **1993**,*26*, 2234-2239

94. P. Beadle and S. P. Armes S. Gottesfeld, C. Mombourquette, R. Houlton, W. D. Andrew and S. F. Agnew *Macromolecules* **1992**, *25*, 2526-2530

95. L. S. Van Dyke and C. R. Martin *Langnuir* **1990**, *6*, 1118-1123

96. Z. Cai, J. Lei, W. Liang, V. Menon, and C. R. Martin *Chem. Mater.,* **1991**, *3(*5), 960

97. R. V. Parthasarathy and C. R. Martin *Chem. Mater.* **1994**, *6*, 1627-1632

98. Z. Cai and C. R. Martin *J. Am. Chem. Soc.* **1989**, *111* , 4138-4139

99. W. Liang and C. R. Martin *J. Am. Chem. Soc.* **1990**, *I 12,* 9666-9668

100. B. W. Maynor, S. F. Filocamo, M. W. Grinstaff, and J. Liu *J.Am. Chem. Soc* **2002**, *124(4)*, 522

101. B. W. Maynor, J. Li, C. Lu, and J. Liu *J.Am. Chem. Soc* **2004**, *126*, 6409-6413

102. O. Schneegans, A. Moradpour, L. Boyer and D. Ballutaud *J. Phys. Chem. B* **2004**, *108*, 9882-9887

103. G. Agarwal, R. R. Naik, and M. O. Stone *J.Am. Chem. Soc* **2003**, *125*, 7408-7412

104. Y. Li, B. W. Maynor, and J. Liu *J. Am. Chem. Soc.* **2001**, *123,* 2105-2106

CHAPTER 2

ATTEMPTED POLYANILINE SINGLE MOLECULE GROWTH USING ELECTROCHEMICAL DIP-PEN NANOLITHOGRAPHY

2.1: Introduction

Conducting polymers (CP) have come up as useful alternatives to the conventional inorganic semiconductors in electronic devices applications due to their ease of processing. Integrated circuits are built from many silicon-based components such as transistors. As the miniaturization of the components of integrated circuits continues, the thin silicon dioxide dielectric layer (which acts to insulate the voltage electrode from the current-carrying electrodes in a transistor), would then reach a limit where it cannot be reduced anymore. Some are already predicting the end of the road for silicon-based transistors [1, 2] due to this limitation. Conventional conjugated polymers have a high resistivity and so are mainly insulators or semi-conductors. However, it was shown that chemical doping increased the conductivity of polyacetylene by more than 10 orders of magnitude [3, 4], although still a semi-conductor. Chemical doping is brought about by chemical methods or by electrochemical oxidation or reduction, among others.

A number of methods have been reported for synthesizing these conductive polymers. Electrochemical polymerization [5, 6] is one of the most commonly used methods. Usually a three-electrode cell is used, with the auxiliary electrode well separated from the working and the reference electrodes. The choice of the working electrode must be such that it does not oxidize with the monomer. Most reported studies have used gold or platinum, while other working electrodes such as graphite and indium tin oxide have also been used. In addition, the solvent of choice should be such that it is a weak nucleophile, if the mechanism of reaction proceeds via radical cation intermediates.

Using polymer precursor route [7-10], a polymer precursor is first synthesized with conventional chemical methods. This precursor is made up of a polymer backbone with pendant, electroactive monomer units. These monomer units are then polymerized

electrochemically on a conducting substrate. A negative bias applied to an AFM tip was also used to polymerize a polymer precursor [11].

E-DPN as an electrochemical method of making CPs using a conducting AFM tip was first demonstrated by Jie Liu and co-workers [12]. Even though at that time there were already some techniques used for fabricating CPs, such as template synthesis and microcontact printing, their severe limitation was patterning structures less than 100nm. Now template synthesis can fabricate nanowires of a few nanometers. As with other DPN techniques, there is formation of a water meniscus at the AFM tip, which facilitates the transport of materials from the tip to the substrate. An electrochemical reaction, in which the negatively biased tip is the anode and the substrate is the cathode, is thus set up and immobilizes the CP on the surface on a path dictated by the movement of the tip [13].

In this study, we present the results leading up to an attempted patterning of conductive polyaniline using the E-DPN method. The aniline was to be delivered by gas phase using N_2 as carrier gas onto a conductive AFM tip for patterning onto mixed monolayers of octadecanethiol and 4-aminothiophenol.

2.2: Experimental

2.2.1: Chemicals

Aniline (99.8%, ACS grade, ACROS Organics, NJ) was used to create polyaniline, 4-aminothiophenol or 4-ATP (Aldrich Chem. Inc., WI), octadecanethiol, or ODT (Aldrich Chem. Inc., WI.) were used to form self-assembled monolayer Au substrates. Potassium ferricyanide ($K_3Fe(CN)_6$, Regent grade, Caledon labs, ON) was used to test the passivating properties of the ODT self assembled monolayer. Concentrated sulfuric acid (H_2SO_4, 96.5%, EMD Chemicals Inc., Germany) and perchloric acid ($HClO_4$, 70%, EMD chemicals Inc., Germany) were used as the electrolyte for aniline. When H_2SO_4 was mixed with 30% hydrogen peroxide (H_2O_2, EMD Chemicals Inc., Germany) in 3:1 ratio, it is called "piranha" and was used for cleaning the Au substrates (CAUTION: piranha is highly corrosive, use with care). A homemade Ag/AgCl/ $KCl_{(sat)}$ reference electrode and Pt wire auxiliary electrode were used in all electrochemical measurements. Nitrogen gas was used to purge

electrochemical solutions and to dry substrates. An 18MΩ cm distilled and deionized water (Barnstead) was used for rinsing substrates and preparing aqueous solutions.

2.2.2: Instrumentation.

All topographic images were obtained using a Nanoscope IV controller and a Dimension 3100 scanning probe microscope (Veeco Inc.). Nanoman software (Veeco Inc.) for creating nanometer-sized patterns on a substrate was used in the scratching of a polycarbonate disk and anodic oxidation of silicon.

Cyclic voltammograms were acquired using a 263A potentiostat (Princeton Applied Research). A conventional three-electrode cell was employed. In all cases, the working electrode was either bare gold or a SAM-modified gold substrate (O-ring area being $0.785cm^2$) and the counter-electrode used was a coiled Pt wire. The reference electrode was a homemade Ag/AgCl electrode saturated with KCl and all values of the applied potential are reported with respect to this reference electrode. Purging with nitrogen gas for 15mins prior to electrochemical measurements deoxygenated solutions.

Infrared spectra were acquired using an ATI Mattson Infinity Series FTIR Spectrometer (Madison, WI) equipped with Mercury-Cadmium-Telluride detector (MCT) cooled with liquid nitrogen. All spectra were acquired at $2cm^{-1}$ resolutions and 500 scans were averaged together to obtain a single spectrum, and all sample spectra were ratioed to a reference spectra of deuterated octadecanethiol.

2.2.3: Preparation of Gold-coated substrates

Microscopic glass slides were cleaned in piranha (CAUTION: piranha is highly corrosive, use with care) for ~30mins. These were then rinsed with copious amounts of deionized water and dried with nitrogen gas. The clean slides were loaded into a thermal evaporator system (Torr Int'l Inc. NY). A 15nm adhesive layer of Cr was first deposited and then 200nm of Au. These Au slides were then stored in plastic slide-mailers approximately one to two weeks.

2.2.4: Preparation of Self-assembled monolayers:

Octadecanethiol SAM: 1mM solution of octadecanethiol in ethanol was prepared in a glass jar. The Au substrates were cleaned using UV ozone cleaner (UVO-

Cleaner®, Jetlight Company Inc.) and then immersed in the ODT solution for 2 ½ days. The substrates were then rinsed with ethanol and dried with N_2 gas.

4-aminothiophenol (4-ATP) SAM: 1mM solution of 4-ATP in ethanol was prepared in a glass jar. Au substrates cleaned as above were immersed in the 4-ATP solution for 2 ½ days. The substrates were then rinsed with ethanol and dried with N_2 gas.

Mixed monolayers of ODT and 4-ATP: A mixed monolayer solution of ODT and 4-ATP with a total thiol concentration of 1mM was prepared in ethanol. Au substrates cleaned as described above were immersed in the mixed monolayer solution for 2 ½ days. The substrates were then rinsed with ethanol and dried with N_2 gas.

2.2.5: FTIR measurements:

Absorbance spectra were acquired using 500 scans for both the background and sample at a resolution of $2cm^{-1}$ while allowing ~15 minutes for purging the system after loading both background and sample. The background spectra were each subtracted from the sample spectra, Fourier-transformed and baseline-corrected.

2.2.6: Electrochemical measurements:

In all cases, a conventional three-electrode cell was assembled, with an exposed geometric area, defined by the size of an O-ring, of $0.785cm^2$. About 5mL of the sample solution was used. The set-up was connected to the computer-controlled potentiostat and the measurements made.

2.2.7: AFM Studies:

2.2.7.1: Scratching of Polycarbonate disk

A tapping mode tip (Digital Instruments, CA) was loaded onto the cantilever holder, which was then mounted onto the end of the scanner head. The laser was adjusted onto the cantilever while also adjusting the photodetector. The tip was then engaged onto the polycarbonate disk used as a substrate for the experiment. A lithographic macro written for this purpose was used to direct the tip and systematically vary the tip translation rate and Z-distance at some pre-set incremental values. The Z-distance between the tip and substrate was optimized for the best scratching.

2.2.7.2: Anodization of a doped Silicon substrate

A Cr/Au-coated tip (Veeco Instruments, CA) with a tune frequency of 323 KHz was loaded and laser aligned on it. A boron-doped Si wafer was used as the substrate. Using the Nanoman software on the Dimension 3100 microscope, voltages ranging from -3 to -8V were applied to the tip at different Z-distances and tip velocity of 50nm/s. The scan size was 10microns. The oxidized structures formed were then imaged using tapping mode.

2.3: Results and Discussion:

The use of Infrared spectrometry served a dual purpose: one was to characterize the substrate and two, in the process also to verify the integrity of the SAM molecules. The IRRAS spectrum in Figure 2.1 is that of a SAM of octadecanethiol (ODT) on Au substrate. The ODT was used to block any electron transfer between the Au substrate and the aniline monomers during polymerization.

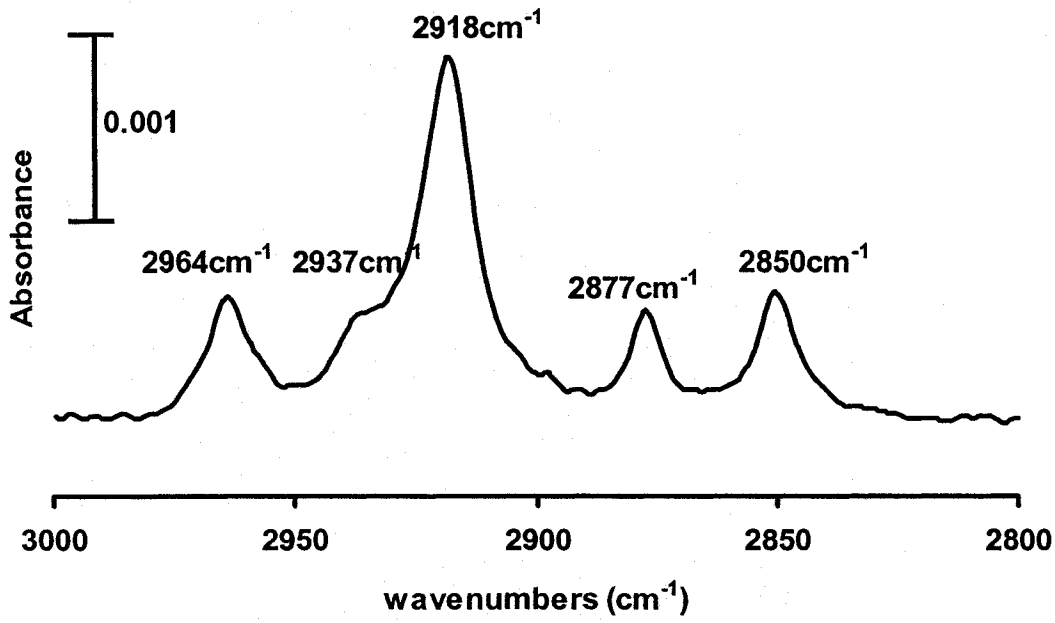

Figure 2.1: IRRAS spectrum of a SAM of ODT in ethanol on Au substrate after 2 ½ days of immersion.

The band at 2964cm^{-1} is assigned to the CH_3 asymmetric in-plane CH stretching mode and the ones at 2937cm^{-1} and 2877cm^{-1} are the CH, symmetric CH stretching mode, (split due to Fermi resonance interactions with the lower frequency asymmetric CH); while the peaks at 2918cm^{-1} and 2850cm^{-1} are the asymmetric and symmetric CH_2 stretching modes respectively [14-16].

Porter *et al* [14] showed that the exact position of these peaks indicates that long-chain alkane thiols are crystalline-like and indicates the alkyl tails are fully extended with all-trans conformation compared with those of short-chain alkanes that tend to have a more disordered liquid-like structure. The intensity of the CH_2 stretching mode absorption is directly related to the number of CH units per alkyl group.

The long immersion times were just for convenience. Studies have shown that by approximately 3hrs for 1mM solutions of ODT, a well-ordered crystalline SAM has already been formed [16].

In order to test for defects within the SAM of ODT on Au, cyclic voltammetry of a 1mM $K_3Fe(CN)_6$ in 1M $HClO_4$ was carried out. Such blocking experiments using diffusing solution species like $Fe(CN)_6^{3-}$ provides very useful information about the electron transfer barrier properties. In all of the cyclic voltammograms, the potential becomes more negative to the right of the X-axis while the positive (cathodic) current is up the positive Y-axis.

Figure 2.2 is essentially featureless and clearly indicates that the ODT monolayer was very effective in passivating the surface and thus blocking any electron transfer between the Au and the $Fe(CN)_6^{3-}$. Most of the observed current is capacitive current. This capacitive behavior resembles the theory of the electrical double layer that models the electrochemical interface as an ideal capacitor.

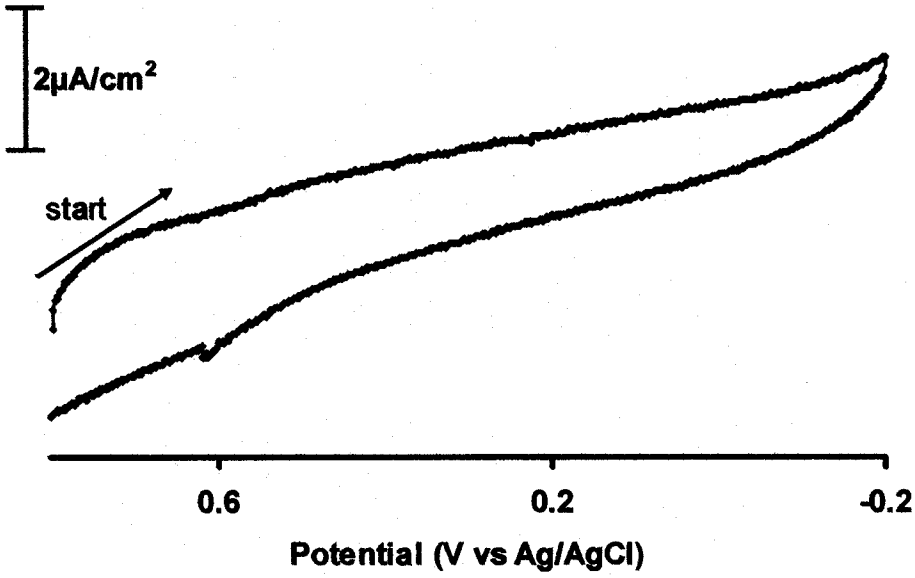

Figure 2.2: The cyclic voltammogram of 1mM $K_3Fe(CN)_6$ in 1M $HClO_4$ on an ODT modified Au substrate. Two cycles were acquired at 100mV/s. Solution was purged with N_2 gas for ~15mins.

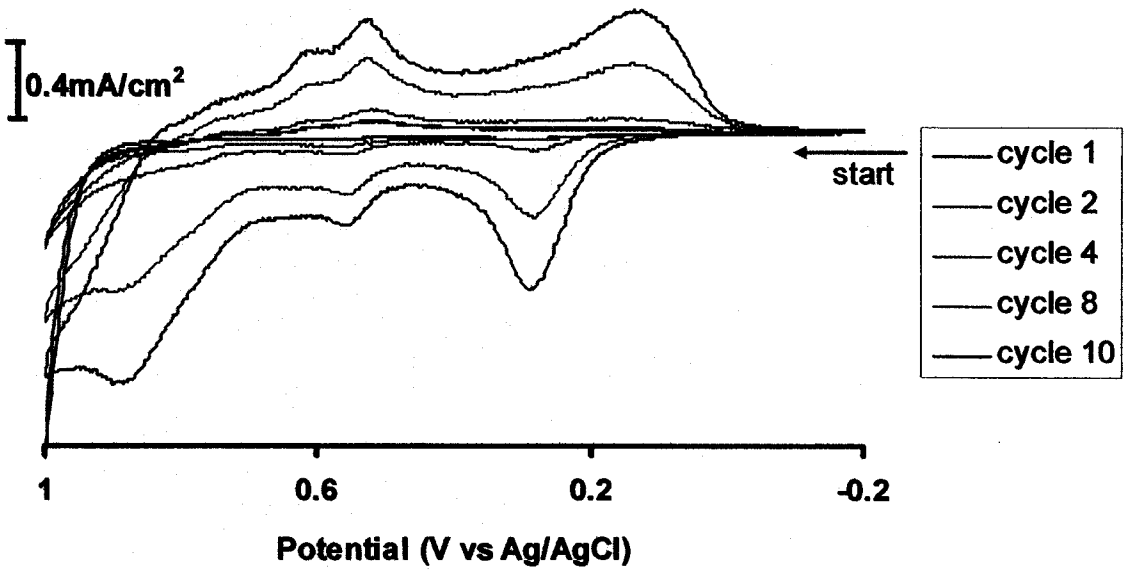

Figure 2.3 shows the CV for the formation of polyaniline on bare Au using 0.02M aniline in 0.5M H_2SO_4. Ten cycles were run at 20mV/s

With bare Au, there should not be any electron transfer barrier for the polymerization of aniline. The CV in Figure 2.3 is for the polymerization of aniline on bare gold. The data shows redox processes at 0.29V (anodic scan) and 0.1V (cathodic scan) corresponds to anion doping and dedoping on the electrodeposited polyaniline (PANI) film and is responsible for the dramatic change in its conductivity. The redox processes at 0.55V (anodic) and 0.52V (cathodic) corresponds to the removal and insertion respectively, of protons in the PANI film [17]. While on bare gold, aniline was polymerized to form polyaniline (PANI), the data in Figure 2.4 confirms the blocking of electron transfer from the gold substrate onto the aniline monomer by the ODT on the surface, and the fact that there are probably very few defects within the ODT monolayer.

4-ATP is an aromatic amine that was to be used to selectively polymerize aniline on an ODT-modified gold substrate. Immersing a gold substrate in a 1mM solution for a period of 2 ½ days made a monolayer of 4-ATP. Cyclic voltammetry and IRRAS were used to characterize the monolayers formed (Figures 2.5 and 2.6). The IRRAS spectrum obtained is shown below in Figure 2.5. The spectra show three characteristic peaks of 4-ATP observed at 1480 cm^{-1} and 1590 cm^{-1} for C-C stretching and 1620 cm^{-1} for N-H bending modes. This IRRAS data confirmed the surface modification of the substrate by 4-ATP.

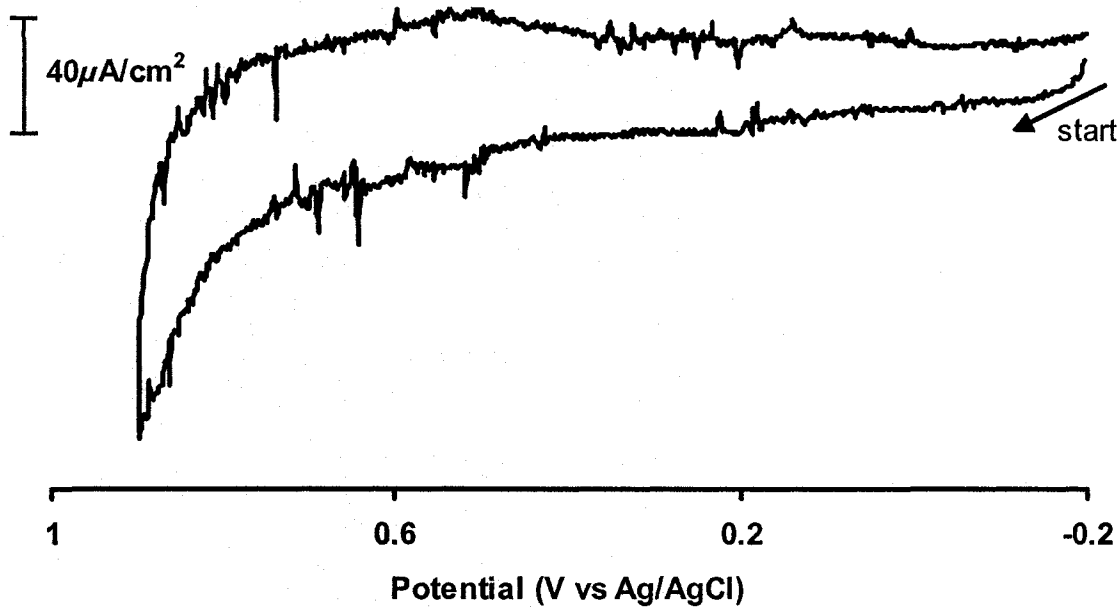

Figure 2.4 shows the tenth cycle of the CV for the polymerization of 0.1M aniline in 0.5M $HClO_4$ on an ODT modified gold substrate. The scan rate used was 100mV/s with 15mins of purging with N_2.

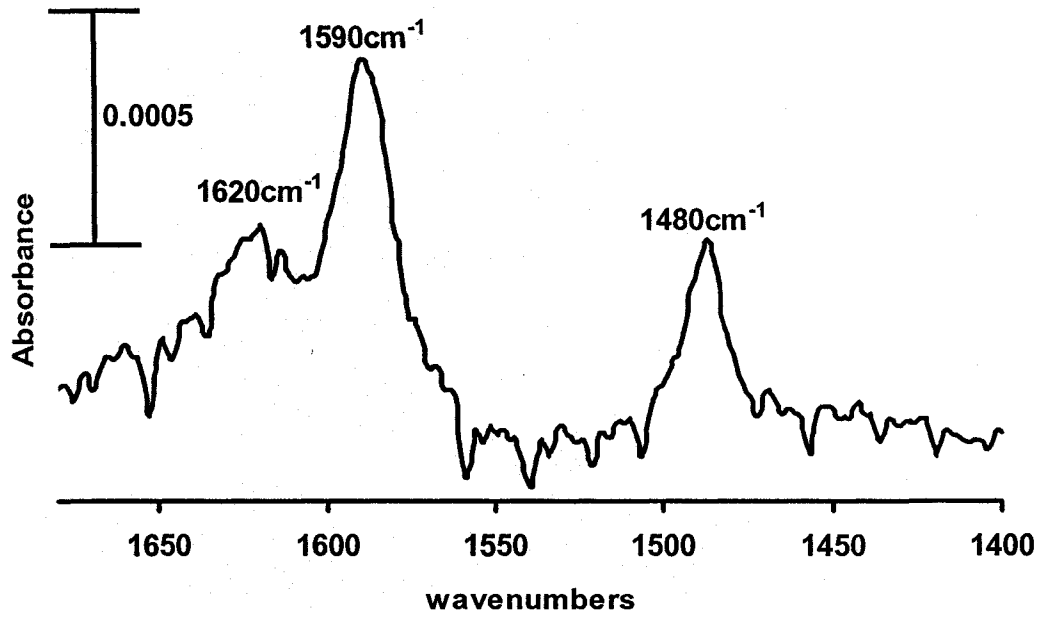

Figure 2.5 is the IRRAS spectra obtained from a 4-ATP monolayer on Au prepared by immersing the gold substrate in a 1mM ethanolic solution for 2 ½ days

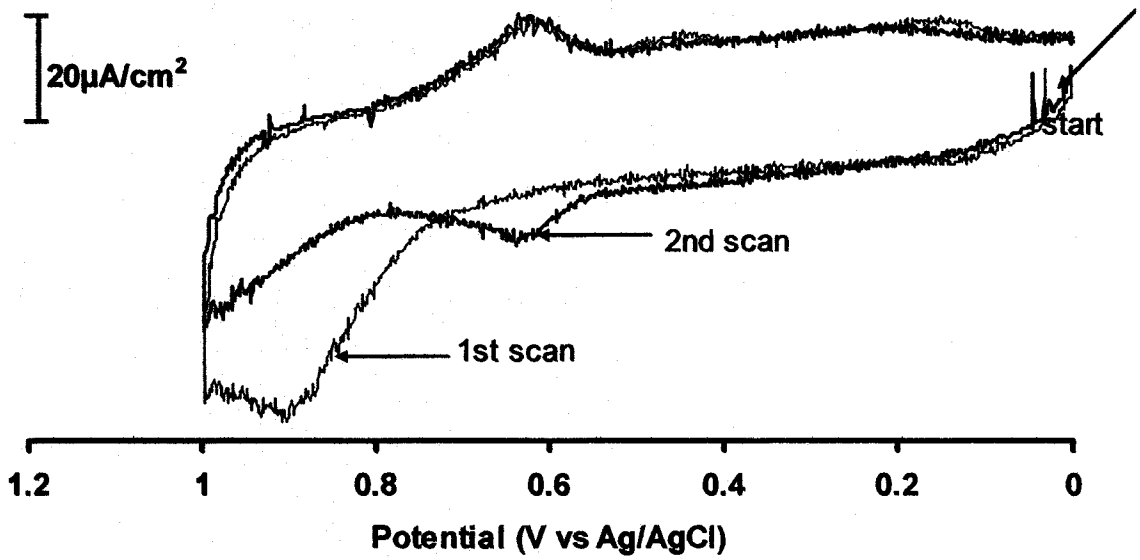

Figure 2.6 shows the electrochemical behavior of 4-ATP monolayer adsorbed on a gold substrate. The electrolyte used was 1M $HClO_4$, with a scan rate of 100mV/s. The first and second scans are shown.

The electrochemical behavior of the adsorbed 4-ATP on gold also served to confirm the success of the modification process. According to Shannon and Hayes [18], the large anodic current peak (0.9V) in the first scan in Figure 2.6 is assigned to the oxidation of adsorbed 4-ATP in its protonated form to the radical cation, which then reacts with a neighbouring 4-ATP molecule to form an adsorbed dimmer. The dimmer is quite strained and is hydrolysed by water to form the final product having a quinone moiety. This quinone moiety gives rise to the reversible peaks at ~0.62V and ~0.64V, while the transient peak at ~0.45V is due to the coupling of desorbed phenazine molecules. The mechanism proposed is shown in Figure 2.7 below

Having confirmed the successful modification of the gold substrate by the 4-ATP, aniline monomers were then polymerized on the modified electrode. Since the oxidation of solution phase aniline occurs at a more positive potential than that of adsorbed 4-ATP, it is possible to initiate the polymerization of aniline at a 4-ATP modified electrode if the electrode is held is held at the oxidation potential of 4-ATP. In Figure 2.8, the anodic oxidative peaks around 0.3V and 0.85V are characteristic of the voltammetric response of polyaniline.

Aniline has now been shown to polymerize on a 4-ATP modified gold electrode. A series of mixed monolayers of 4-ATP and ODT were then prepared in ethanol in order to selectively polymerize aniline on 4-ATP molecules contained within ODT monolayers. The solutions contained different fractions of 4-ATP: 35%, 65% and 90% 4-ATP. IRRAS was used to characterize the resulting substrates and the spectra obtained are shown in Figure 2.9.

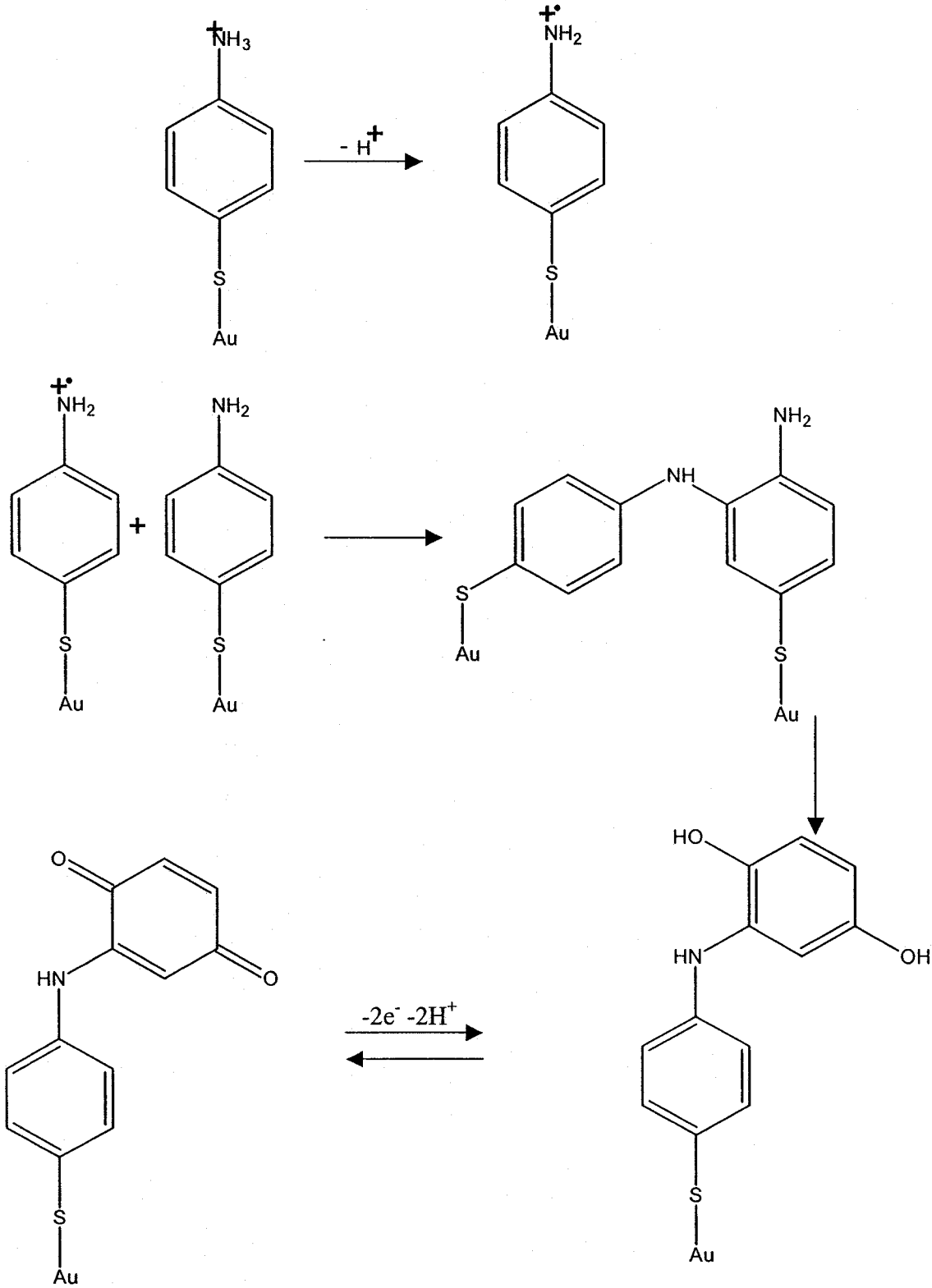

Figure 2.7 shows the proposed mechanism: Oxidation of the adsorbed 4-ATP gives rise to a cation radical, which then couples with a neighbouring 4-ATP molecule to yield a strained dimmer. This is then partially desorbed from the surface and hydrolyzed to yield a quinine species

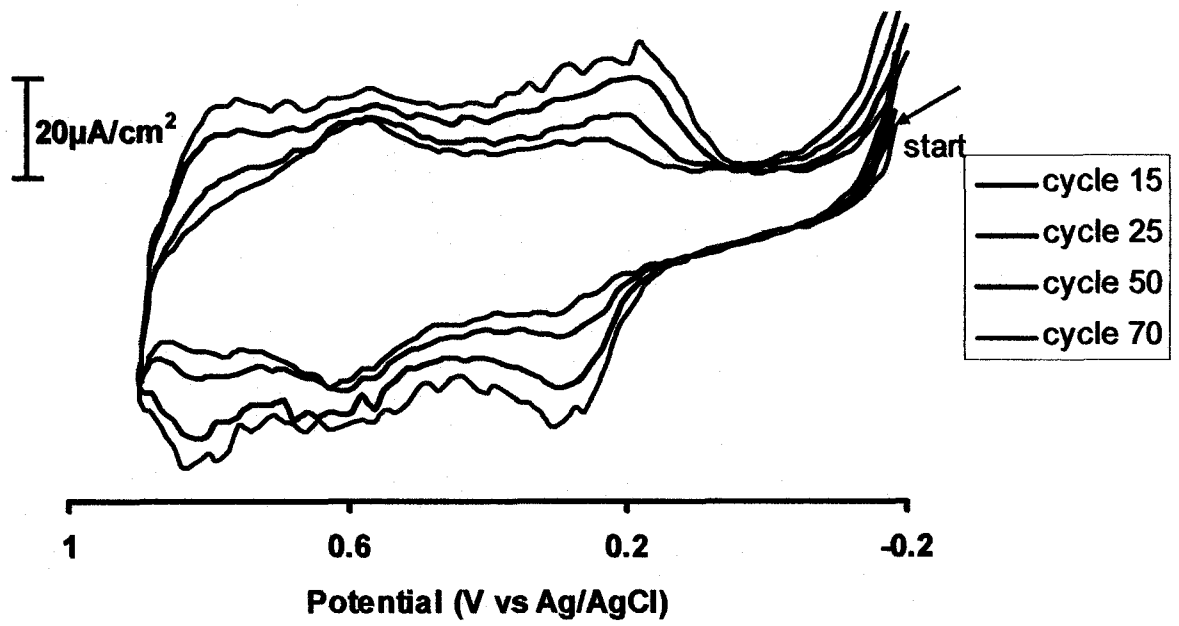

Figure 2.8 shows the polymerization of 0.01M aniline in 0.5M $HClO_4$ on 4-ATP modified Au substrate. The potential was scanned from -0.2 to 0.9V at a rate of 100mV/s. The cycles shown are the 15^{th}, 25^{th}, 50^{th} and 70^{th}.

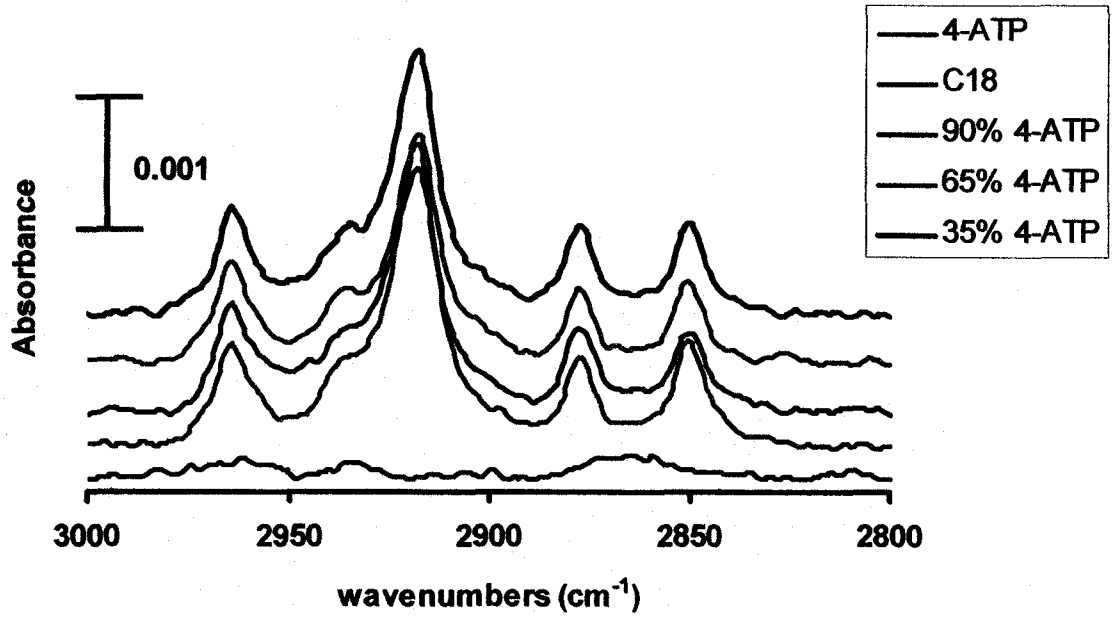

Figure 2.9 shows the IRRAS spectra for pure ODT, pure 4-ATP and the mixed monolayers: 35%, 65% and 90% 4-ATP. Total immersion time was ~60hrs.

As can be observed from the spectra, the pure 4-ATP has no absorption within the range shown since there are no $-CH_2$ and $-CH_3$. As expected, there is no difference in intensities between pure C18 monolayer and those with fractional amounts since the peak intensity is dependent on the number of C-chains. But Shannon *et al* [20] found that there is a shift in the asymmetric CH_2 stretch at 2918cm^{-1} to higher frequencies. Studies have shown that the structure of thiols do not change significantly when immersed in 1mM solutions for more than 18 hours but the coverage increases with extended immersion times which means the number of defects in the SAM decreases. However, in their work, Crooks *et al* [19] found that at long exposure times of an Au substrate in a solution of short-chain and long chain thiols, the resulting SAM contained only the long chain thiol. The ~60 hours used to form the SAM might have resulted in only or predominantly ODT monolayer formed on the surface.

The polymerization of aniline on these mixed monolayers was carried out. The CV obtained is shown in Figure 2.10 below. As can be seen, there was no aniline polymerization due probably to the fact that the length of assembly time was long, therefore giving rise to a predominantly monolayer of ODT being formed.

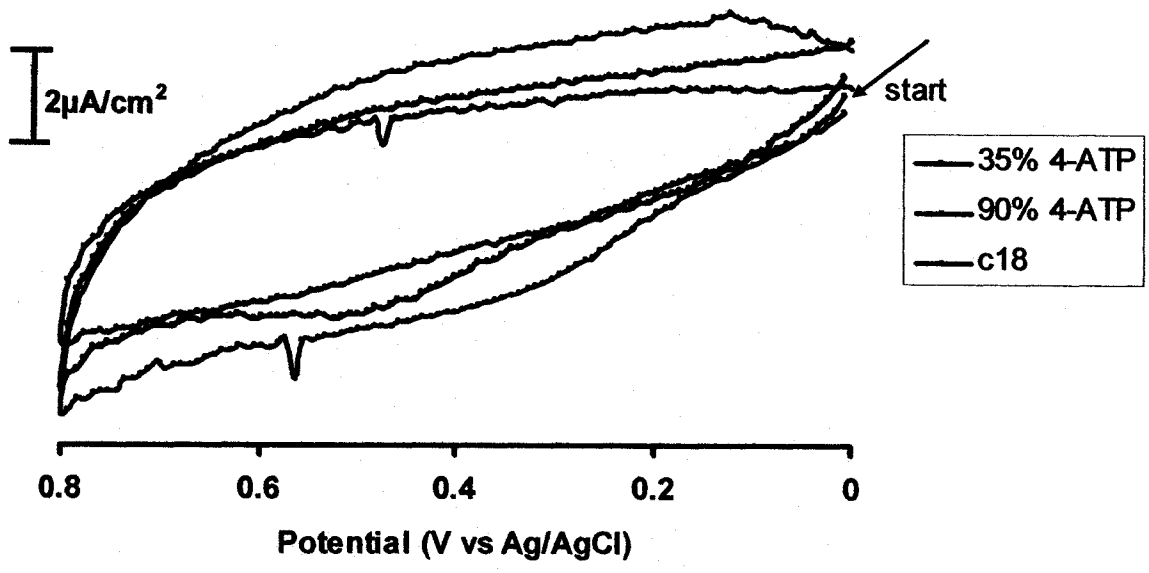

Figure 2.10 shows the 10th cycle each of the cyclic voltammogram of 0.1M aniline in 0.5M HClO4 on mixed SAMs and ODT. The SAMs were assembled from a mixed ODT and 4-ATP solution for ~60hrs.

2.3.2 AFM results and discussion

2.3.2.1 Scratching of Polycarbonate disk

Before starting with the use of the conducting AFM, it was very important to have a feel for the use of the Nanoman software. The software was the same software that would eventually be used for the electrochemical dip-pen nanolithography of aniline. Using the Dimension 3100 training notebook as guideline, a tapping mode tip was used to make scratches on the surface of a polycarbonate disk. By controlling the tip movement manually, the image in Figure 2.11 below was obtained. All the images shown here have been flattened.

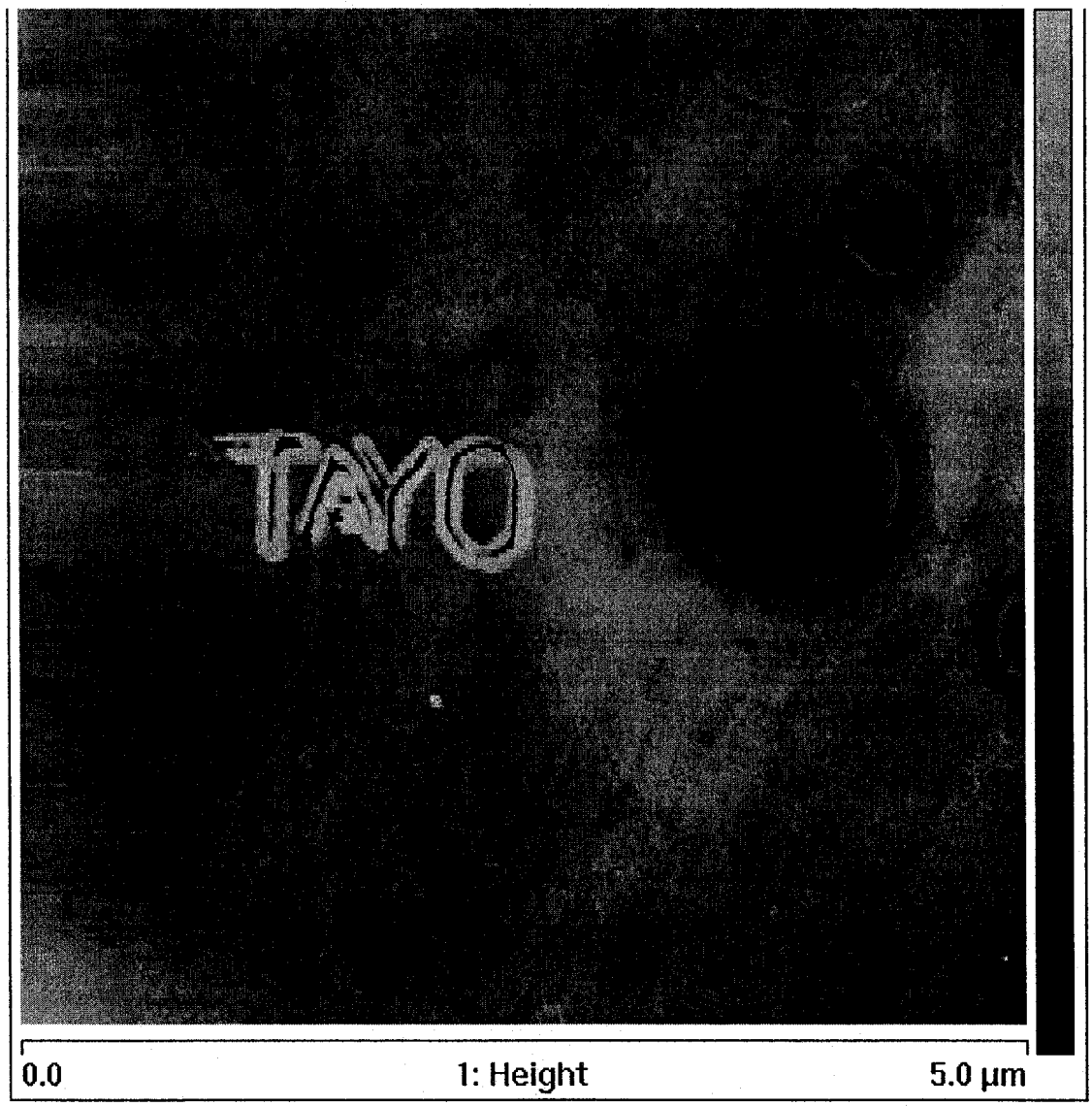

Figure 2.11 is a 5um image obtained by manually directing the tip movement. 512 samples/line was used with 256 lines.

Then the automated control in the Nanoman software was used to create a diamond design on the polycarbonate disk. Here we varied the distance between the tapping mode tip when engaged and the substrate (Z-distance), and the velocity with which the tip scratches the disk. The negative values for the Z-distance means the tip moved from the engaged position towards the substrate. Figure 2.12 was the image obtained.

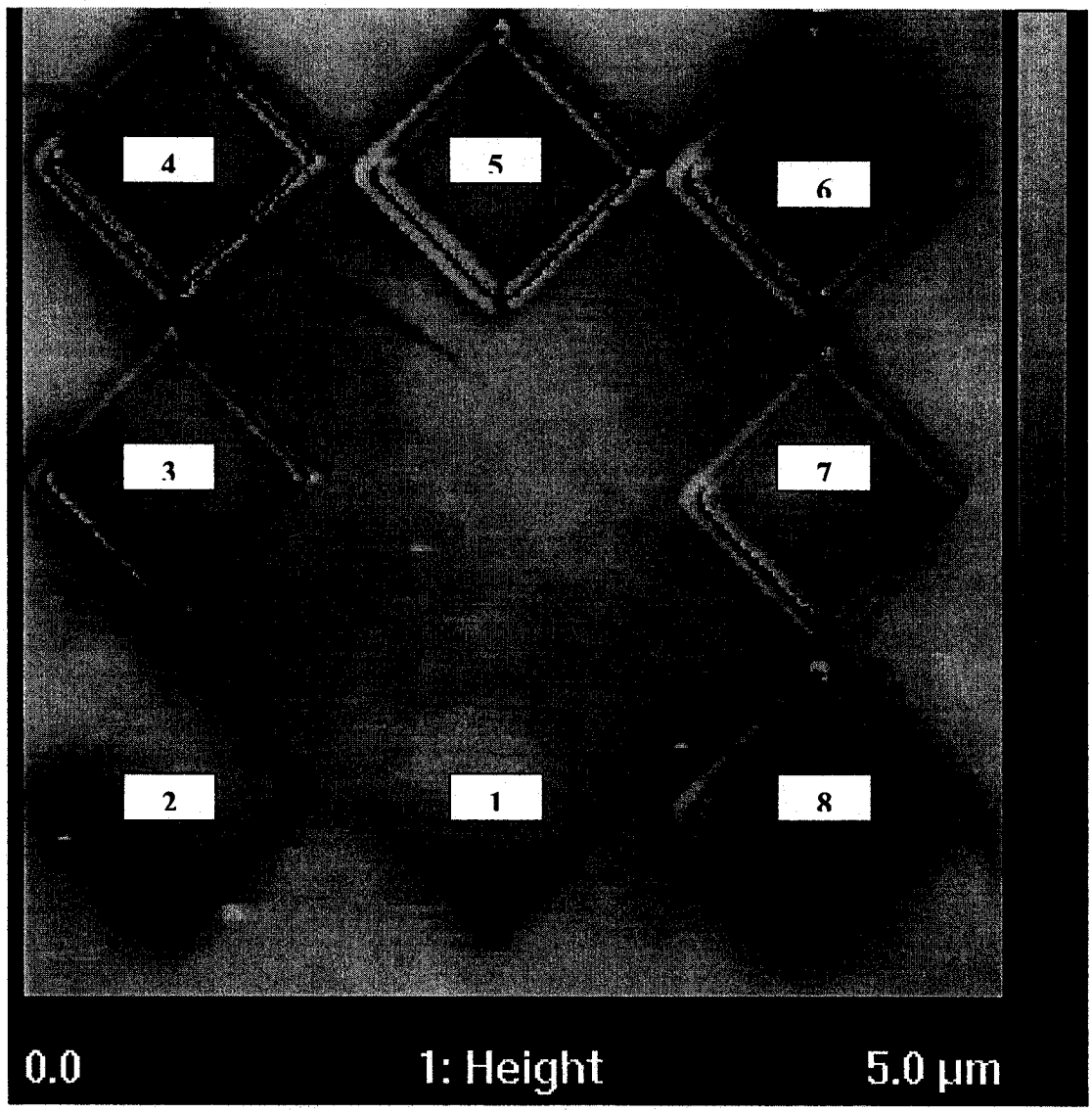

Figure 2.12 shows the image obtained by varying the Z-distance and tip velocity.

Image number	Tip velocity (nm/s)	Z-distance (nm)
1	50	-20
2	50	-30
3	50	-40
4	50	-50
5	40	-50
6	30	-50
7	40	-40
8	50	-50

Table 2.1 shows the data extracted from Figure 2.12

Figure 2.12 suggests that while it appeared the two tip velocities used worked fine, the more the Z-distance, the deeper the scratches made, as should be expected.

Then we wrote a program in C++ using the lithographic commands provided for the instrument that would enable complete automation of the scratching process. The Z-distance and tip velocity were varied in increamental steps during the scratching. The image in Figure 2.13 below was obtained.

Here is a description of the programmed movement of the tip. First, there are 16 blocks of lines. Each of those is made up 11 lines. Each individual line begins at a point A shown on Figure 2.13 for each block set. The parameters here were the Z-distance set at -50nm and the tip velocity set at 1μm/s. The tip then moves up 2μm in Y, 0.2μm in +X, down in Y by 2μm and 0.2μm in +X and so on until the 11^{th} line, which would be up in Y. The tip then moves up in the Z-distance, translates down 2μm in Y and 1μm in +X in order to begin with the next block of lines (B).

For the set B block of lines, Z-distance was changed to -60nm while rate remains at 1μm/s. The 11 lines were then made as block A. Blocks C and D were similarly made, tip velocity remaining 1μm/s but the Z- distance was -70nm and -80nm respectively. After block D, the tip translated a total of11μm in –X and -5nm in –Y to a new position E. For position E, the tip velocity became 2μm/s and Z-distance went back

to -50nm. Blocks E to H were all at same tip velocity but Z-distance went to -60, -70 and -80nm. The next sets of 4 blocks (I-L) were at tip velocity of 3μm/s (Z-distance was -50 to -80nm) and the last set (M-P) at 4μm/s (Z-distance was -50 to -80nm).

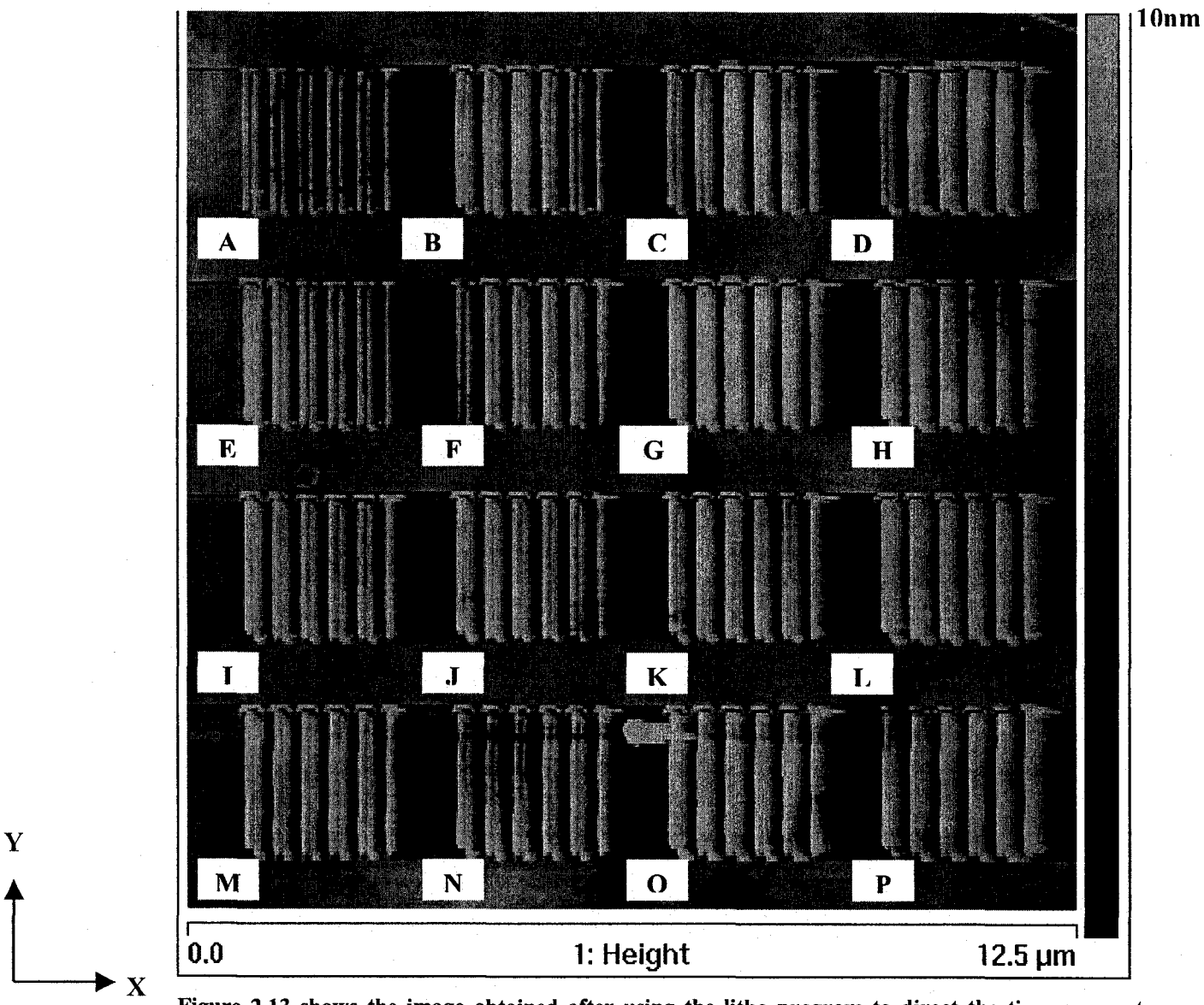

Figure 2.13 shows the image obtained after using the litho program to direct the tip movement during the scratching of the polycarbonate disc

The tip moved across the surface in this pre-programmed pattern, with increasing Z-distance and tip velocity. The higher the Z-distance (the deeper the tip goes into the substrate), the deeper the scratches made. In addition, Figure 2.13 seems to suggest that as the tip moved faster (higher tip velocity), the scratches were even deeper.

2.3.2.2 Anodic oxidation of Silicon

The next experiment was the anodic oxidation of doped silicon. In the experiment, there is the added applied voltage parameter, in addition to the Z-distance and the tip velocity. A conducting, Cr/Au tapping mode tip was used. A voltmeter was used to verify the applied potential applied to the tip. Figure 2.14 shows the image obtained when the doped silicon was imaged before the oxidation and it reveals a very flat silicon surface.

In Figure 2.15, the image obtained after the anodic oxidation of the doped silicon is presented. The applied voltage and Z-distance were varied while keeping the tip velocity constant at 50nm/s.

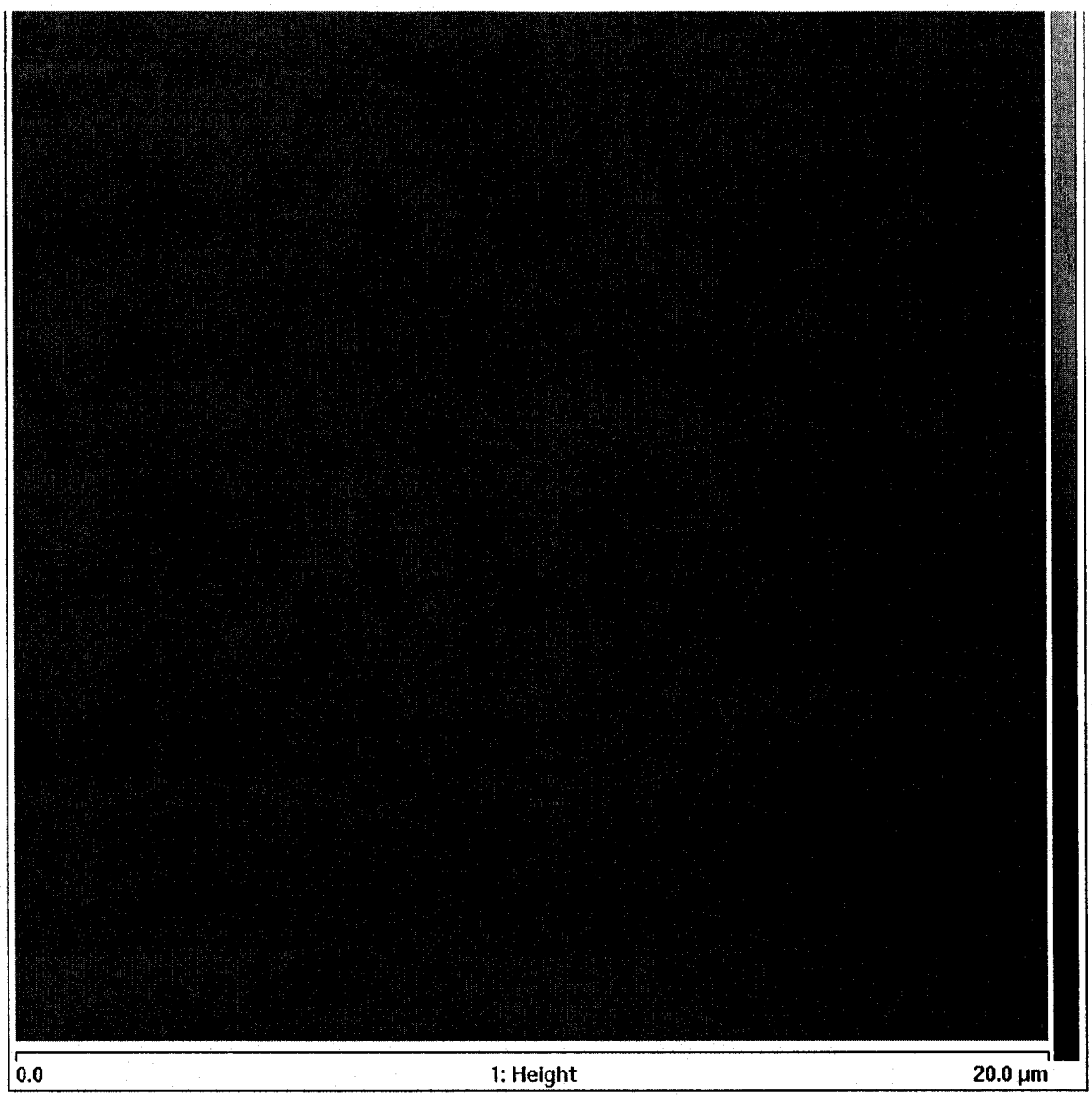

Figure 2.14 shows the doped Si before lithography. The scan rate used was 1Hz

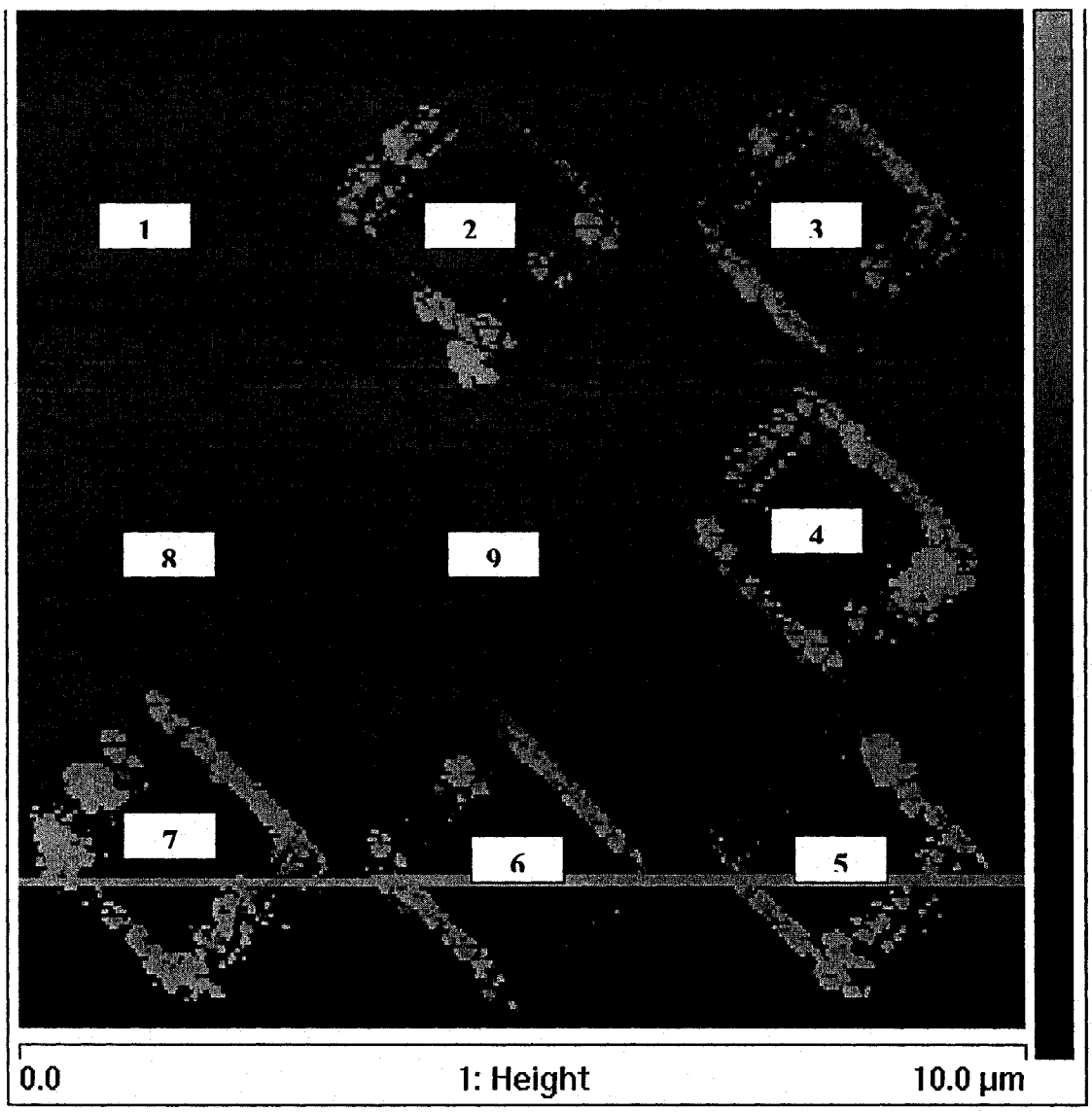

Figure 2.15 shows the doped Si after the anodic oxidation. The voltage applied to the tip was between -3 to -8V. The scan rate used was 1Hz for the imaging.

Image number	Applied voltage (V)	Z-distance (nm)
1	-5	-10
2	-5	-20
3	-5	-30
4	-5	-40
5	-6	-40
6	-7	-40
7	-8	-40
8	-4	-40
9	-3	-40

Table 2.2 shows the data extracted from Figure 2.15

Some observations worthy of note in Table 2.2 are 1) at lower applied voltages to the tip (-3V and -4V), there was no oxidation observed while using -5V to -8V there was oxidation of the silicon; 2) a Z-distances of -40nm seems to be optimal while at a Z-distance of -10nm, no oxidation was observed.

The original idea was to use electrochemical dip pen nanolithography to polymerize aniline from gas the gas phase on a mixed monolayer of ODT and 4-ATP. The Glass shop of Chemistry department here built a manifold, which is made up of four glass flasks and two flow meters. Only one of the flasks would be used, and it would contain a dilute solution of aniline in water. Using one of the flow meters, N_2 gas is fed into the tube to generate bubbles and some gaseous aniline molecules. Using the second flow meter, another stream of N_2 is used to transport the generated gaseous molecules to the AFM tip. Data obtained using UV visible spectroscopy (data not shown) confirms the presence of aniline.

Using the above set up however, would only result in only a certain concentration of aniline at the AFM tip at any certain time. Firstly, we decided to do a study where the concentrations of both aniline and the dopant ion (using H_2SO_4) were varied. In order to avoid mixing of the solutions at different concentrations, polydimethylsiloxane (PDMS) stamp with holes would be used. Reports from literature

indicate that PDMS should be extracted in organic solvents before use in order to get rid of unpolymerized molecules that could end up contaminating the substrate. This was the point where the second project actually began.

2.4 References:

1 D. A. Muller, *Nature,* **1999,** *399,* 758-761

2 M. Schulz *Nature* **1999**, *399,* 729-730

3 H. Shirakawa, E. J. Louis, A. G. Macdiarmid, C. K. Chiang, and A. J. Heeger *J.Chem.Soc. chem. comm.*, **1977**, *16*, 578-580

4 Y. Furukawa *J. Phys. Chem.* **1996**, *100,* 15644-15653

5 C. N. Sayre and D. M. Collard ***Langmuir 1996,*** *11,* 302-306

6 S. Inaoka and D. M. Collard *Langmuir* **1999,** *15,* 3752-3758

7 C. Xia, X. Fan, M. -k. Park, and R. C. Advincula *Langmuir* **2001**, *17,* 7893-7898

8 P. Taranekar, X. Fan, and R. Advincula *Langmuir* **2002**, *18,* 7943-7952

9 C. Xia and R. C. Advincula *Chem. Mater.* **2001**, *13,* 1682-1691

10 S. Deng and R. C. Advincula *Chem. Mater.* **2002**, *14,* 4073-4080

11 S. Jegadesan, R.C. Advincula and S. Valiyaveettil Adv. Mater. **2005**, *17*, 1282-1285

12 Y. Li, B. W. Maynor, J. Liu, *J. Am. Chem. Soc.* **2001**, *123*, 2105-2106

13 S.-Y. Jang, M. Marquez, G. A. Sotzing *J. Am. Chem. Soc.* **2004,** *126*, 9476-9477

14 M. D. Porter, T. B. Bright, D. L. Allara, and C. E. D. Chidsey *J. Am. Chem. Soc.* **1987,**

109, 3559

15 S. A. John, T. Ohsaka *Journal of Electroanalytical Chemistry* **1999**, *477* 52–61

16 A. Jakubowicz, H. Jia, R. M. Wallace, and B. E. Gnade *Langmuir* **2005,** *21,* 950-955

17 W.-S. Huang, B. D. Humphrey and A. G. MacDiarmid *J. Chem. Soc. Faraday Trans.*

1, **1986**,*82*, 2385-2400

18 W. A. Hayes and C. Shannon *Langmuir* **1996**, *12*, 3688-3694

19 O. Chailapakul and R. M. Crooks *Langmuir*, **1995**, *11*, 1329

20 W.A. Hayes, H. Kim, X. Yue, S. S. Perry and C. Shannon *Langmuir* **1997**, *13*, 2511-2518

CHAPTER 3

CHARACTERIZATION OF CONTAMINANT MOLECULES FROM POLYDIMETHYLSILOXANE

3.1 Introduction

Polydimethylsiloxane or PDMS is the most widely used elastomer in micro-contact printing (μCP) [1, 2] and microfluidic systems [3, 4]. In both cases, there is conformal contact between the polymer and the substrate. During the use of polydimethylsiloxane for micro-contact printing, the presence of PDMS residue has been reported along with the transferred molecules. Buck and co-workers [5] detected some PDMS residue on a gold substrate while attempting to compare the quality of μC-printed hexadecane thiol with that assembled from solution. Since this observation had not been reported before then, it was assumed that it was likely due to the higher pressures used for the printing that resulted in the transfer of the residues.

Ratner and co-workers [6] also reported the transfer of PDMS residue during μCP. Using secondary ion mass spectrometry (SIMS), they found the presence of PDMS residues on an Au substrate and proposed an exhaustive weeklong cleaning of the stamp before use. Glasmastar *et al* [7] however, came up with the most detailed and systematic work on the contamination of substrates by PDMS residue. Using a variety of surfaces, water or buffer were stamped using both flat and patterned PDMS stamps. The results were compared with stamps that had been oxidized with UV/ozone. In all cases where the native, unextracted PDMS was used, there was significant transfer of molecules onto the substrate whereas the treated polymer showed very much reduced levels of contamination.

Over the years, a number of other workers have also observed the transfer of PDMS residues along with the inking molecules during microcontact printing. [8-15]. One detrimental effect of PDMS contamination during μCP was observed by Felmet *et al* [10] in which Cu was deposited on PDMS by e-beam evaporation and then contacted with an octanedithiol modified GaAs substrate. In a similar procedure, Au was also patterned. Surprisingly however, all the printed Au was always conductive whereas printed Cu patterns, regardless of thickness, were never conductive. X-ray

photoelectron spectroscopy (XPS) data later revealed that PDMS oligomers permeated through the entire thickness of printed Cu, resulting in nonconductive patterns.

While most of the reported works regarding PDMS contamination showed the detrimental effects, Bjork and co-workers [16] utilized the hydrophobic nature of the contaminant molecules on a substrate surface to attach and stretch DNA along the direction of fluid flow. Inganas *et al* [17, 18] used the transferred PDMS oligomers to modify the surface energy of a conducting polymer substrate. Still other people found no direct contamination when native, unextracted PDMS stamps [19, 20, 28] were used.

Contamination in microfluidic channels made in PDMS has not been as commonly reported as during μCP. In a study by Whitesides *et al* [22], a piece of flat, native PDMS was extracted using 1-propanol and the extract quantified using ^{1}HNMR. The amount obtained was then compared with the amount extracted when 1-propanol was allowed to flow through a microchannel made from native PDMS. The amount of PDMS contaminant molecules was found to be much smaller through the microchannel because of the smaller surface area of the PDMS in contact with the solvent. The microfluidic PDMS was later cleaned by extraction with pentane and the flow of 1-propanol through the microchannel was repeated. The cleaning resulted in an even smaller amount of PDMS molecules extracted. Based on the above results, it was concluded that contamination from the PDMS microchannel would not be an issue when using extracted PDMS. This study however, did not address the diffusion of PDMS molecules from the microchannel onto the substrate.

Many techniques have been used to study these PDMS residues in solution or on surfaces. Solutions containing extracted PDMS molecules have been studied using ^{1}H NMR [22] and MALDI-TOF-MS [21]; while surface characterization have been achieved using XPS [7, 24], TOF-SIMS [6, 13, 25], FTIR [15, 17, 27]

Pre-treatment of the PDMS is the only way reported so far of reducing the level of contamination from PDMS molecules. The use of ultraviolet (UV), ultraviolet/ozone (UVO) [7, 27], oxygen plasma [29, 30] and corona discharge [31, 32] to change the surface properties of PDMS from hydrophobic to hydrophillic were also found to reduce the amount of transferred oligomers to the substrate. Many other workers reported either extracting or sonicating the PDMS in organic solvents as a means of

removing the uncrosslinked molecules [6, 15, 27]. Extraction with organic solvents has not been shown to modify the surface properties of PDMS, so might be more useful in applications that do not require surface modification of the PDMS. The cleaning method used in this study is that of extraction using a boiling solvent (hexane) rather than cold extraction.

3.2 Experimental

3.2.1: Chemicals

Sylgard 184 silicone elastomer and curing agent (Dow Corning) were used to fabricate polydimethylsiloxane, hexane (98.5%, ACS, EMD Chemicals Inc., Germany), toluene (99.8%, ACS, FisherScientific, NJ), ethylacetate (99.5%, ACS, EMD Chemicals Inc., Germany), acetone (99.5%, ACS, FisherScientific, Canada), and 95% ethanol (industial grade, Winnipeg, MB) were used in the extraction of the contaminant molecules from, and subsequent deswelling of the PDMS. Methanol (99.8%, ACS, FisherScientific, Canada) was used to extract the extracted PDMS molecules from hexane for electrospray (ESI) analysis. Tetrakis(trimethylsilyloxy)silane (Alfa aesar, MA) was used as a caliberation standard for ESI analysis. When H_2SO_4 (95-98%, ACS, EMD Chemicals Inc., Germany)was mixed with 30% hydrogen peroxide (ACS, H_2O_2, EMD Chemicals Inc., Germany) in 3:1 ratio, it is called "piranha" and was used for cleaning the Au substrates (CAUTION: piranha is highly corrosive, use with care). An 18MΩ cm distilled and deionized water (Barnstead) was used for rinsing substrates. Purified N_2 using a 0.2μm filter (Millipore, Ireland) was used to dry all samples.

3.2.2: Instrumentation

All infrared spectra and mapping data were acquired on a Vertex 70 spectrometer equipped with a microscope (Bruker Optics) and liquid nitrogen-cooled Mercury-Cadmium-Telluride (MCT) detector. In all the studies, KBr (potassium bromide) beam-splitter was used. Unless otherwise stated, a grazing angle objective was used under constant nitrogen flux to purge the system of carbon dioxide and water vapor. A $2cm^{-1}$ resolution was used in all the studies.

The instrument used for acquiring XPS data was an Axis-Ultra spectrometer (Kratos Analytical) with a vacuum base pressure of $5x10^{-10}$ torr. The x-ray source used

was Al Kα with initial photon energy 1486.71 eV, operated at power of 210W. The angle between the sample and the analyzer (take-off angle) was 90°. The x-ray beam-spot diameter was about 1mm. Survey spectra were acquired at pass energy of 160 eV, within a binding energy range 0-1100eV, in step increments of 0.33 eV. For the high-resolution spectra, pass energy was 40 eV, in step increments of 0.1 eV. The pass energy determines the resolution of the spectra, the higher the pass energy, the lower the resolution and vice-versa.

Extracts of the PDMS in hexane were analyzed using Matrix-Assisted Laser Desorption/Ionization on a time of flight (MALDI/TOF-MS) mass spectrometer (Applied Biosystems). Positive ion spectra were acquired in a reflectron mode. Dihidroxy benzoic acid (DHB) matrix in tetrahydrofuran (30mg/mL) was mixed in a 5:1 ratio with the sample. Polyethylene glycol (molecular weight 3500) was used to calibrate the time of flight system in order to obtain accurate masses. Flow injection analysis was performed on a single quadrupole instrument equipped with electrospray ionization interface (Agilent Technologies).

3.2.3: Preparation of gold-coated substrates.

Glass microscopic slides were cut into appropriate sizes (when necessary) and cleaned using "piranha" (CAUTION: piranha is highly corrosive, made from concentrated sulfuric acid and 30% hydrogen peroxide in a 3: 1 ratio) for ~30mins. These were then rinsed with copious amounts of deionized water and dried with purified N_2. The clean slides were loaded into a thermal evaporator system (Torr Int'l Inc. NY). Approximately 5nm adhesive layer of Cr was first deposited, followed by ~200nm of gold. These gold slides were then stored in plastic slide-mailers for up to a week.

3.2.4: Fabrication of PDMS

A 10:1 (w/w) mixture of the elastomer base and curing agent respectively, were thoroughly mixed for 15mins and then degassed in a vacuum dessicator for 45mins. The degassed mixture was then poured out on a cleaned Si wafer to cure at room temperature. Curing time was always 24hrs unless otherwise stated. After curing, the

PDMS was peeled off and cut into varying sizes depending on the intended use. In all cases where PDMS was used to print on a surface, no inks were used.

3.2.5: Characterization of PDMS extracts

PDMS was prepared as described above but left to cure for ~40hrs. For each extraction, two 50 x 10mm pieces were placed into 400mL boiling hexane (67°C) for 3hrs. The PDMS was deswelled back to the original size in a vacuum dessicator. This extraction step was repeated three times. The extract was poured onto a beaker and left to evaporate in the fume hood until the solution was ~4mL. A solution of each of the two starting materials – the elastomer base and curing agent – was prepared in hexane and used as controls. The extracted samples, the solutions of the starting materials and pure hexane were then analyzed by MALDI/TOF MS.

For flow injection analysis, 50μL of the hexane extract was mixed with 2mL of methanol before running the analysis. Tetrakis(trimethylsilyloxy)silane was used as the calibration standard (the structure is shown in Figure 3.2). 20μL sample was injected. Flow solvent used was 100% acetonitrile at 0.60mL/min. Positive ion spectra was acquired in scan mode.

3.2.6: Distance-dependence study of contaminant molecules using XPS

A 50mm x 10mm piece of gold-coated substrate was cleaned in piranha. A (25mm x 10mm x 2mm, *lwh*) piece of flat, native PDMS was cut out and two holes 5mm diameter and 5mm apart were cut into it. The PDMS was placed on the gold substrate such that about half the surface area of the gold had contact with the PDMS while the other half was not in contact with the PDMS, (Figure 3.1) for 2hours. A line was drawn demarcating the PDMS contact areas from non-contact areas. A gold substrate that was taken through the same "piranha" cleaning process but without any PDMS contact was used as a control. Both were mounted in the vacuum chamber of the XPS instrument for analysis.

3.2.7: Distance-dependence study of contaminant molecules using FTIR

A gold-coated microscopic slide (3″x1″) was cleaned in piranha. A piece of PDMS was brought into contact with the gold substrate for 2hrs. A line was drawn close

to the edge of the PDMS in order to demarcate between the contact and the non-contact areas. The gold substrate was then mounted under the 15X objective of the Vertex 70 microscope and snapshots taken in order to determine how much distance the line actually was from the edge of the PDMS at a certain defined point. After 2hrs, the PDMS was carefully peeled off the substrate. The contact and non-contact areas on the gold substrate were mapped and spectra collected with the grazing angle objective of the FTIR microscope.

3.2.8: Time-dependence study of contaminant molecules

Pieces of PDMS were brought into contact with cleaned Au substrates for 10, 30 and 120mins. The ~10 x 25mm pieces were cut from a bigger piece of PDMS cured on a silicon wafer for 24 hours. After contact for the specified times, the Au substrate was analyzed using the grazing angle accessory of the FTIR microscope. Only the non-contact areas were analyzed, starting from the points at the edge of the contact area with the PDMS to about 10mm away.

3.2.9: Mechanistic study on the mode of transfer of contaminant molecules

Using the same set-up as in section 3.2.7 above, a second piece of 25 x 15mm Au substrate was brought close to that used above (i.e. the Au substrate with the PDMS), separated by a 300μm wire, for 2hrs. The set-up was such that the PDMS was placed right on one edge of the 3″x1″ Au substrate that was close to the 25 x15 mm substrate. The area from the edge of the 25 x 15mm substrate that was close to the PDMS was then mapped using the grazing angle objective to a distance ~10mm away, and spectra acquired.

3.2.10: Study on PDMS contamination in microfluidic channels

A patterned microfluidic PDMS stamp was fabricated by mixing a 10:1 (w/w) of an elastomer base and curing agent respectively for 15mins and degassing in a vacuum dessicator for 45mins. The mixture was then poured onto a cleaned 1cm^2 silicon master (fabricated by standard photolithographic techniques) having the desired relief structures and allowed to cure for 24hrs at room temperature. The patterned stamp was

peeled off the silicon master and brought into conformal contact with a cleaned gold substrate for 2hrs and later analyzed using FTIR.

A microfluidic channel has a top "ceiling" and then the sides. In order to study how the sides and the "ceiling" contribute to the PDMS contamination of the substrate, two sets of experiments were performed. In the first experiment to study the contribution from the "ceiling", a piece of PDMS was covered with a 13μm thick aluminum foil that had a square (7x7mm) hole. A gold substrate was positioned on top of the assembly for 2hrs such that only vapors from the stamps could reach the gold surface through the square hole in the foil. After 2hrs, the gold substrate was removed from the aluminum foil and analyzed by FTIR. To study the contribution of the PDMS molecules from the sides, PDMS was cured around two 1cm^2 cuvettes in order to make 10 x 10mm holes within the PDMS after cure. These holes also represented sides that were not cut, which is similar to that in a microfluidic channel. The stamp was cured for 24hrs and then brought into contact with a gold substrate for 2hrs. The non-contact areas within the holes were analyzed using FTIR.

3.2.11: Study of cleaning procedures on the extent of contamination from PDMS

Three different methods were used to extract the uncrosslinked molecules from PDMS. These were cold solvent extraction, cold solvent extraction with systematic deswelling of the PDMS and hot solvent extraction. The cold solvent extraction involves immersing the PDMS in hexane overnight, sonicating in a 2:1ethanol / water mixture three times for 15mins each time and then allowing to dry in a vacuum dessicator. The cold solvent extraction with systematic deswelling of the PDMS involves placing the PDMS in hexane for two days, changing the solvent each day. Deswelling the PDMS involves the use of different solvents of increasing polarity. First, immerse in toluene for a day, then ethylacetate the next day and in acetone the third day. Finally, the PDMS was dried in an oven at 90°C for a day. The hot solvent extraction involves extracting the PDMS molecules in 200mL boiling hexane (67°C) for 3hrs. The PDMS was dried in a vacuum dessicator.

3.3: Results and Discussion

3.3.1: Characterization of extracted PDMS molecules

The original drive for this project was to extract the uncrosslinked PDMS molecules from the bulk of the polymer. After a couple of cold extractions of the PDMS using hexane, the idea of trying to quantify the amount of PDMS extracted with each extraction step was conceived. The quantification would help provide an idea about how many extractions are required to achieve a thorough cleaning of the PDMS. The method of choice was gas chromatography coupled with mass spectrometry detection, but after running a sample from a first extraction step that was diluted with hexane 16-fold, the peaks kept eluting from the column long after analysis. This continuous elution would create problems for other users of the instrument. MALDI was then considered.

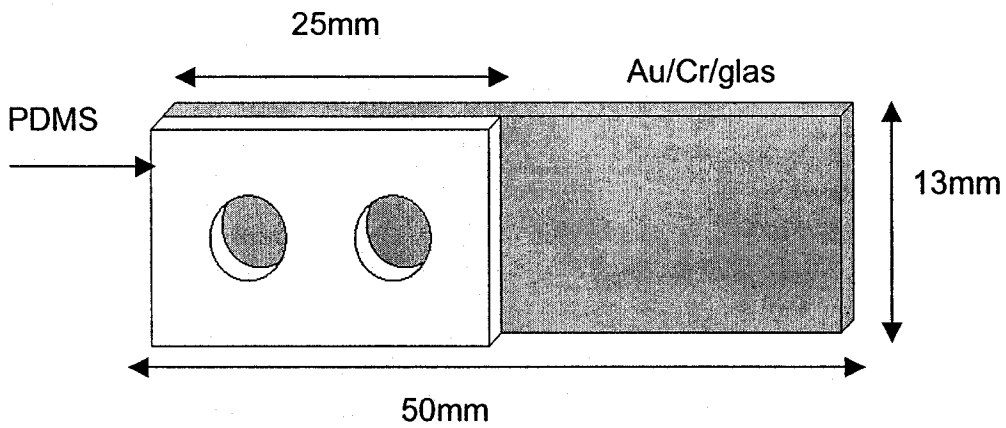

Figure 3.1 The experimental set-up for the XPS measurement. A 25mm piece of native PDMS was brought into contact with a cleaned gold substrate for 2hrs. A line was drawn at the edge of the PDMS to demarcate between contact and non-contact areas.

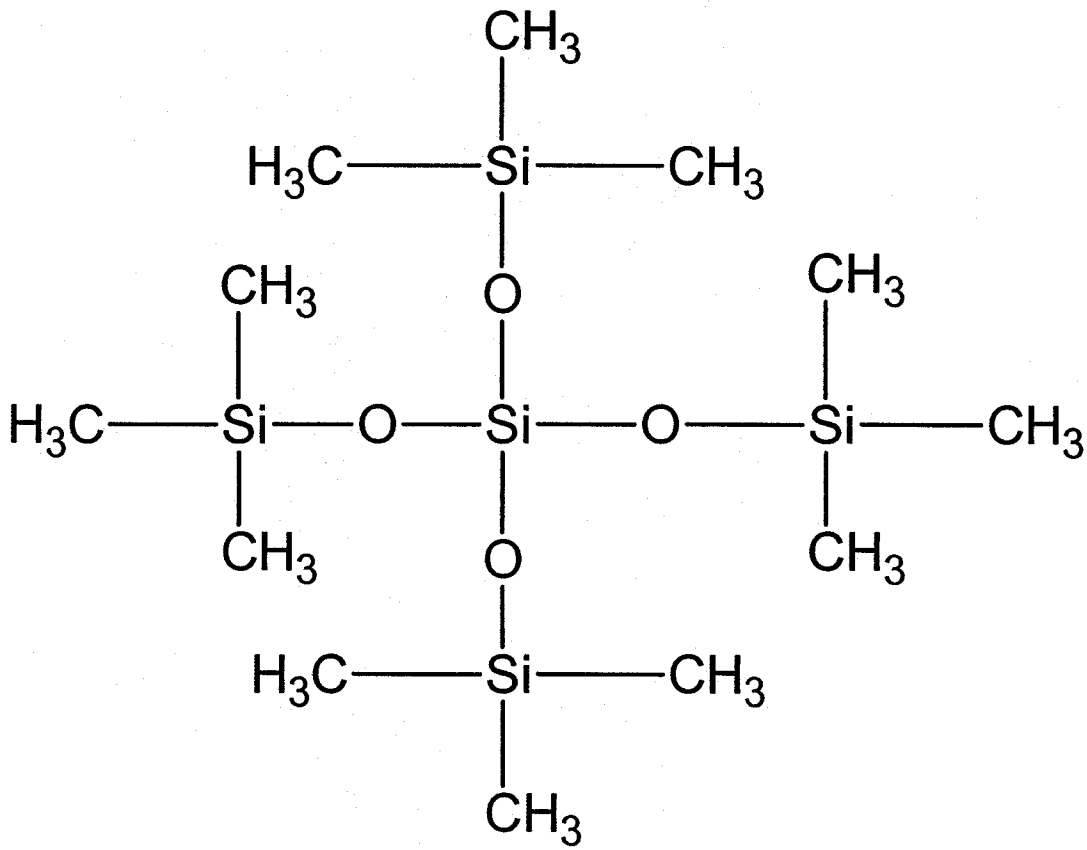

Figure 3.2: The structure of the tetrakis(trimethylsilyloxy)silane calibration standard used in the ESI-MS experiment

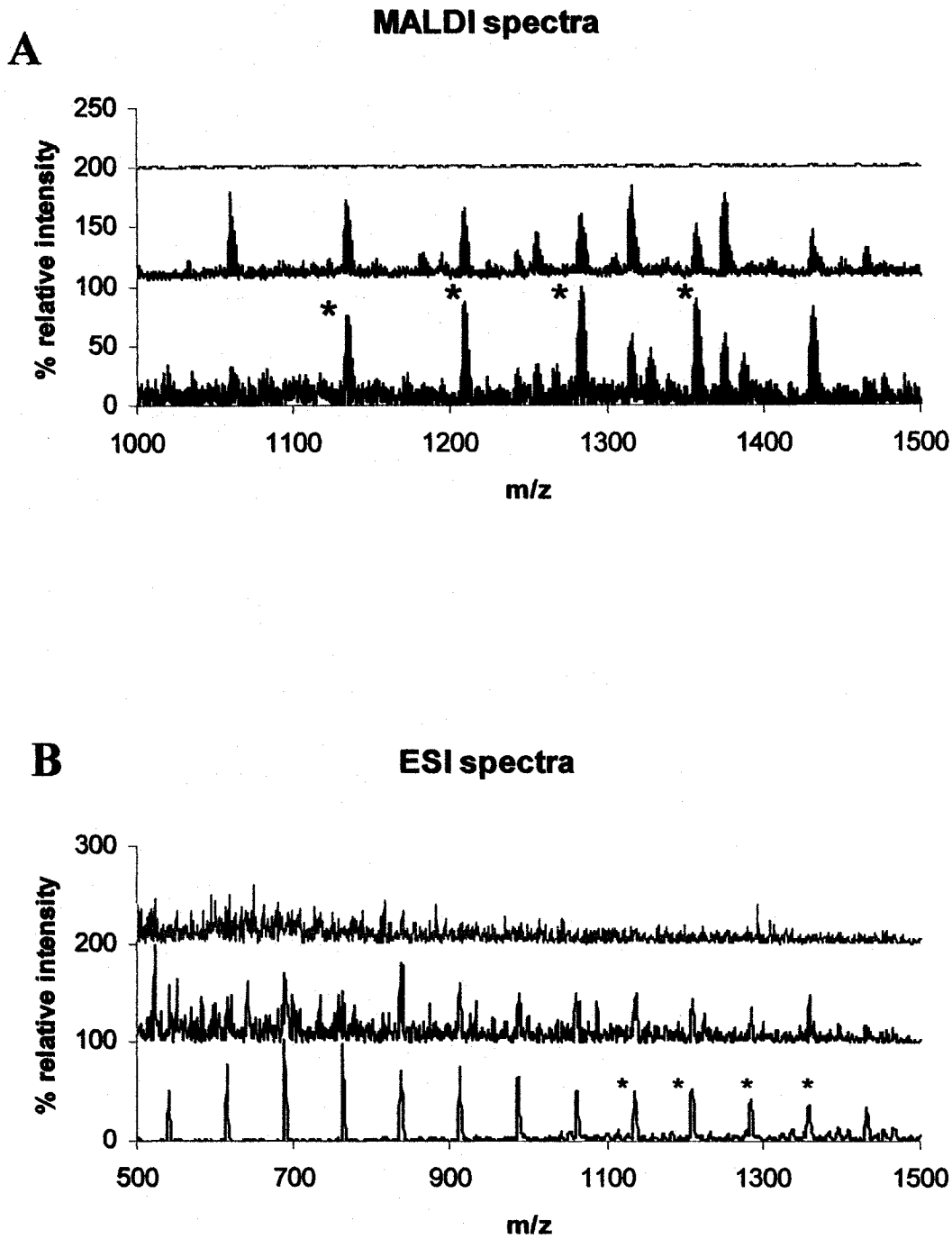

Figure 3.3 A) MALDI spectra of the elastomer base starting material (bottom), the first extract (middle) and the fourth extract in hexane (top); B) ESI spectra of first (bottom), second (middle) and fourth extracts (top) in methanol. Asterisked peaks showed similarity between MALDI and ESI data. Spectra are offset for clarity.

Figure 3.3A and B show the spectra obtained using MALDI and ESI respectively. In the MALDI spectra, there is similarity between that of the base and the samples. This observation may be because the contaminants are mostly from excess uncrosslinked base. Those peaks correspond to the molecular ion peaks of uncrosslinked, low molecular weight molecules possibly attached to a sodium cation. The difference between those peaks in most cases corresponds to 74 m/z, or $SiO(CH_3)_2$, the repeating unit in PDMS [23]. This mass difference is consistent with the structure of one of the components of the base.

The sample peaks <1000 m/z were not observed in MALDI (not shown) probably due to swamping by matrix-adduct peaks, but readily observable with ESI. The MALDI data in Figure 3.3 also shows that the amount of contaminant molecules extracted into the hexanes was decreasing with the number of extractions which is reasonably expected, as less and less amount of the contaminants remained after each extraction. The higher level of background with the increasing number of extraction cycle in ESI is due to the presence of less and less sample.

ESI quantification was not used because the internal standard was difficult to ionize. We tried collecting negative ion spectra, added some sodium acetate to the acetonitrile mobile phase and even tried using atmospheric pressure chemical ionization method, but still there were no recognizable peaks.

3.3.2: XPS diffusion studies

X-ray Photoelectron Spectroscopy (XPS) has found quite a lot of use in surface characterization studies such as in the confirmation of the surface modification of substrates [11], and thickness of thin films [12]. In XPS, electrons are emitted from materials when irradiated with x-rays and their kinetic energies are determined using an energy analyzer. Different chemical species gives specific kinetic energies, which also depends on the chemical environment. While one look at a survey scan is enough to tell what chemical species are present on a surface, high-resolution spectra are useful for quantitative purposes. A typical survey scan and a high-resolution spectrum of a gold substrate that had been in contact with PDMS are shown in Figure 3.4. In all the data presented here, Si2s peaks were used because the Si2p peaks are buried in the large background of Au4f peaks.

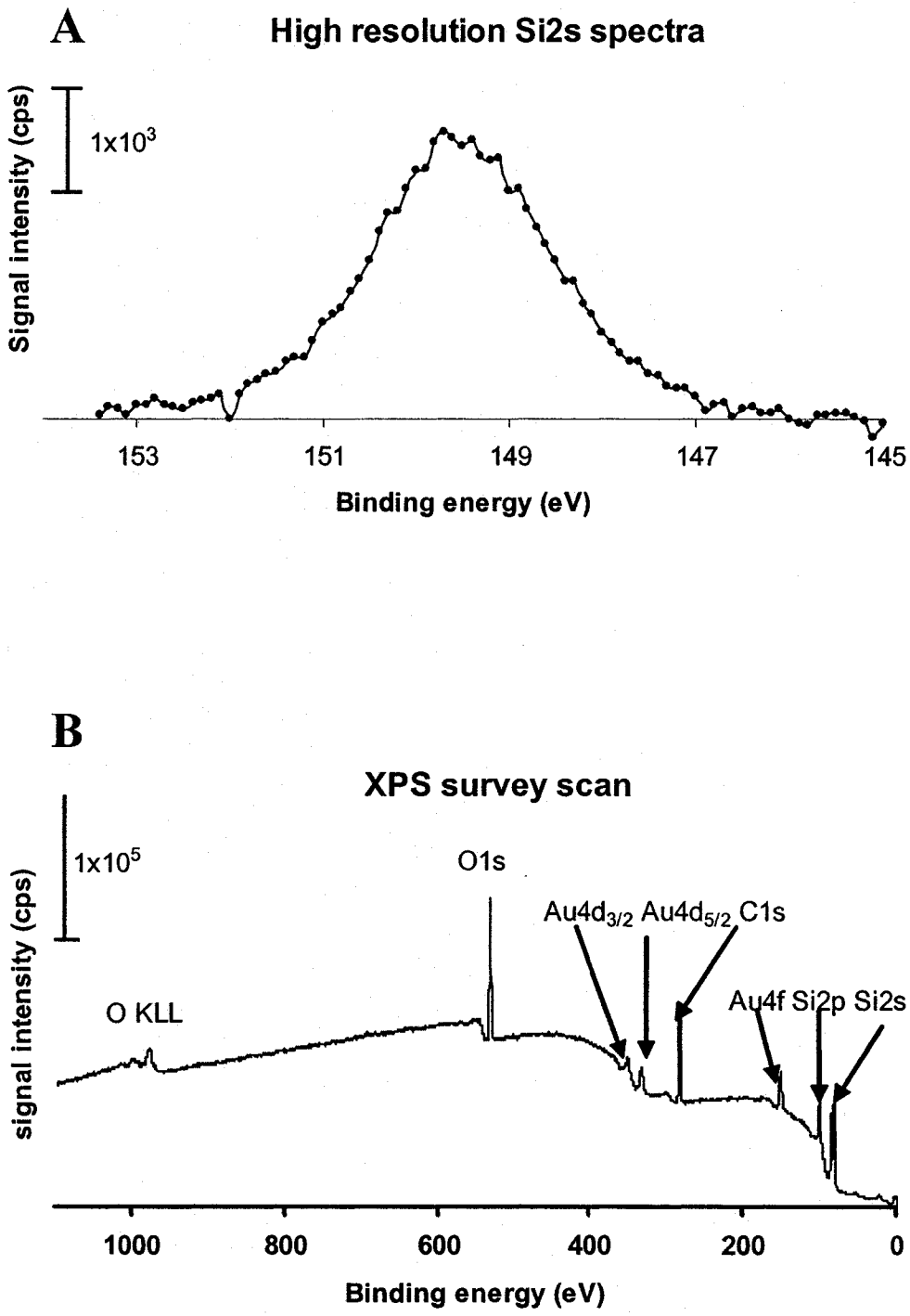

Figure 3.4 (A) is a high resolution Si2s spectra obtained from a point 2mm away from the edge of the PDMS while (B) is a survey scan of the same spot. Beam spot size was ~1mm

Ten different spots within the PDMS contact areas were analyzed, in groups of five spots within a 5mm radius. Since the XPS beam spot diameter was ~1mm, we safely assumed there were no overlaps. Figure 3.5 shows the result obtained for one of the groups using high-resolution Si2s peaks. As can be observed, the spots gave widely varying amounts of PDMS on the gold surface within the area of contact. This inhomogeneity might be because of the uneven crosslinking during the curing process within the bulk PDMS that probably resulted from the mixing process of the elastomer base and curing agent. This results in some areas having more uncrosslinked molecules compared to other areas. We tried our best to ensure thorough mixing such that all the different areas in the bulk of the polymer cure evenly.

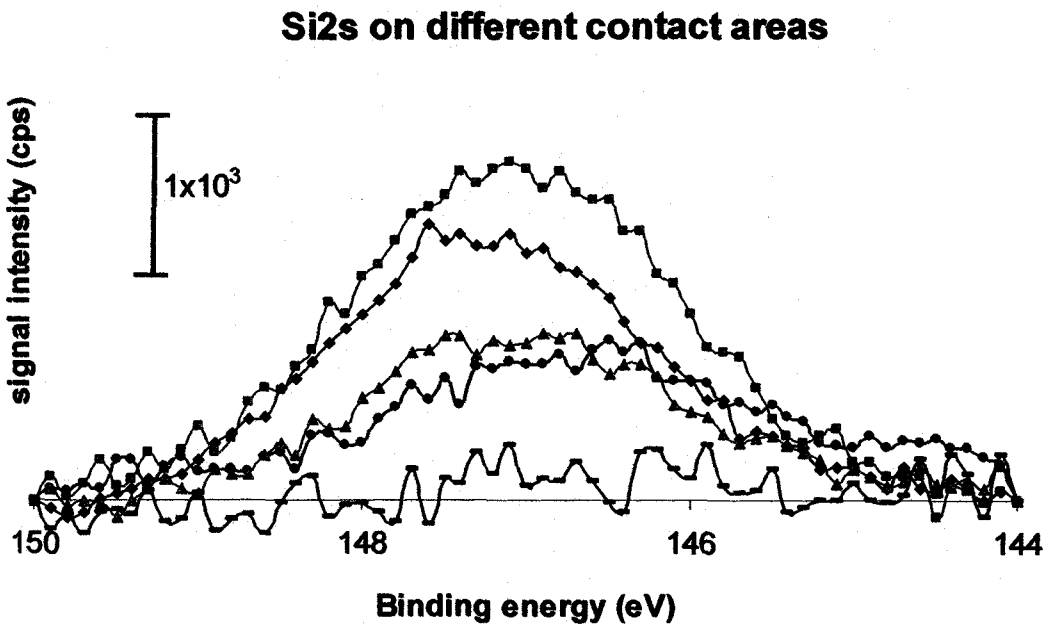

Figure 3.5 High-resolution Si2s spectra acquired from five different spots in an area where PDMS was in conformal contact with the Au substrate. The amount of transferred PDMS varied widely.

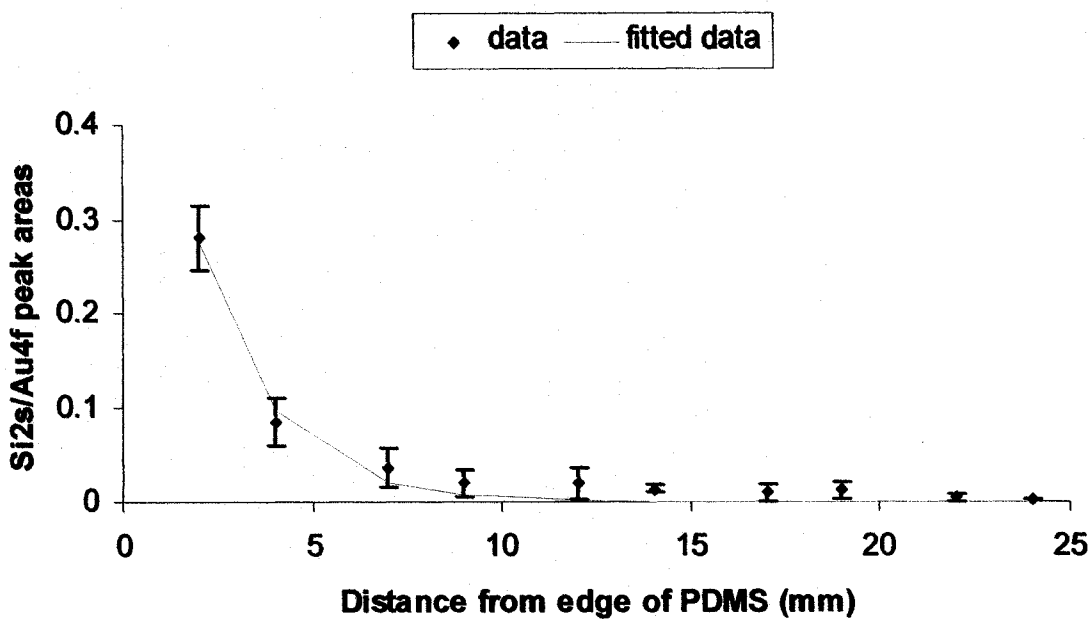

Figure 3.6 is a plot showing the distance dependence of the amount of uncrosslinked molecules transferred from native PDMS onto non-contact areas. The ratio of the peak areas of the Si2s and Au4f peaks from the high-resolution XPS spectra are plotted against the distance away from the edge of the PDMS. The data is an average of two experiments. The curve was fitted to the equation $(y = \exp(-x * a) * b)$ **by least squares method where x=distance and a= 0.531905 and b= 0.802967.**

Now that the transfer of uncrosslinked PDMS molecules in areas where there was conformal contact between the native PDMS and gold substrate has been established, the next question answered was about the distribution profile of these contaminant molecules in regions where there was no PDMS contact. A line was carefully drawn to mark the edge of the contact area of the PDMS on gold. Ten different positions along a 25mm distance from this line were analyzed by XPS. Figure 3.6 gives a result that is quite similar to what was expected.

Figure 3.6 is a plot showing the distance dependence of the amount of PDMS residue transferred onto the gold substrate. The Figure shows that at distances farther away from the area where the PDMS was in contact with the gold substrate, the amount of uncrosslinked molecules transferred from the PDMS to non-contact areas decreased exponentially. No comparison was made between the levels of contamination in non-contact and contact areas because of the inhomogeneous distribution in contact areas.

A similar study has been reported before by Glasmastar *et al* [7]. They observed that for UV/ozone-cleaned PDMS in contact with a gold substrate, more of the

contaminants were predominantly detected in non-contact areas and they proposed that the most likely reason is the escape of those molecules from possible cracks in the brittle-like SiO_x layer formed on the PDMS surface by the oxidation process. This is however the first time that uncrosslinked PDMS molecules would be reported in non-contact areas with native, unextracted PDMS.

Cleaning PDMS twice in boiling hexane (67°C) for 3hrs helped extract these uncrosslinked molecules from the polymer matrix, as shown in Figure 3.7. High solubility solvents such as hexane, [6, 22] are useful in extracting uncrosslinked PDMS oligomers from the bulk of the polymer. Solvent effects on the cleaning of PDMS are further discussed later in this chapter.

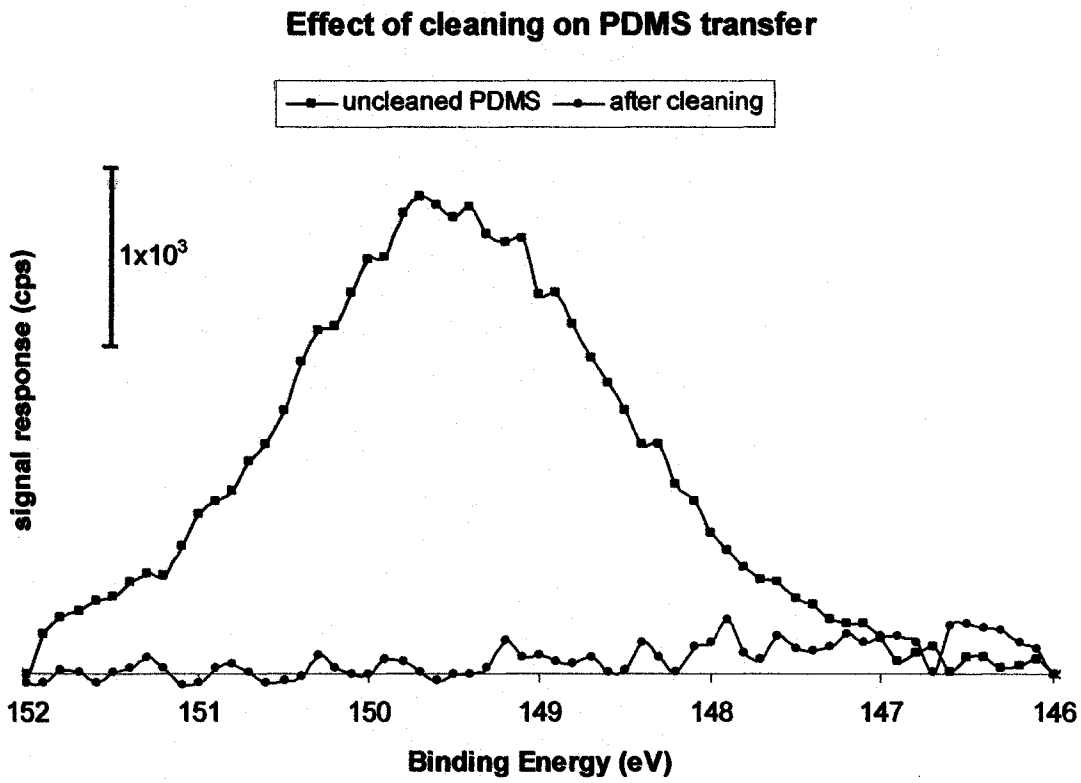

Figure 3.7 compares the XPS spectra acquired on two gold substrates that had contact with native and extracted PDMS. The PDMS was extracted twice in boiling hexane.

We then set about finding out the possible mechanism for the transfer of PDMS molecules across the surface using FTIR. The instrument is equipped with a

microscope, and in addition to the software, can be used to map out designated areas on the substrate from which spectra would be acquired.

3.3.3: FTIR diffusion studies

The first thing that became apparent was the inhomogeneity in the polymer distribution on the surface in areas where PDMS had contact with gold substrate. This observation confirmed the previous XPS data. It seemed that the transfer occurred across the contact surface where there was conformal PDMS contact. The spectra in Figure 3.8 clearly show the (a) asymmetric CH_3 stretch in Si-CH_3 (2990 cm^{-1}- 2940cm^{-1}); (b) symmetric CH_3 deformation in Si-CH_3 (1280 cm^{-1} - 1240 cm^{-1}); (c) asymmetric Si-O stretching in $[-(CH_2)_2\text{-Si-O-}]_x$ (1170 cm^{-1}- 1000 cm^{-1}); and (d) CH_3 rocking and Si-C stretching in Si—CH_3 (820 cm^{-1} - 785cm^{-1}) [23,27]

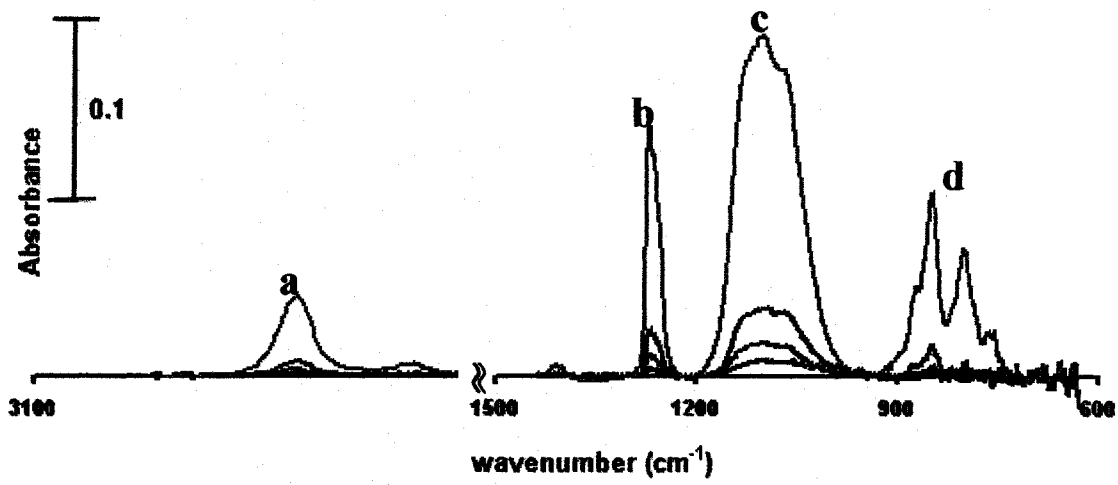

Figure 3.8: Four spectra acquired from different spots all within ~1mm of each other in areas that had PDMS contact. 30scans at 2cm^{-1} resolution was used. The peaks are (a) CH_3 stretch in Si-CH_3, (b) CH_3 deformation in Si-CH_3, (c) Si-O stretching and (d) CH_3 rocking and Si-C stretching in Si-CH_3

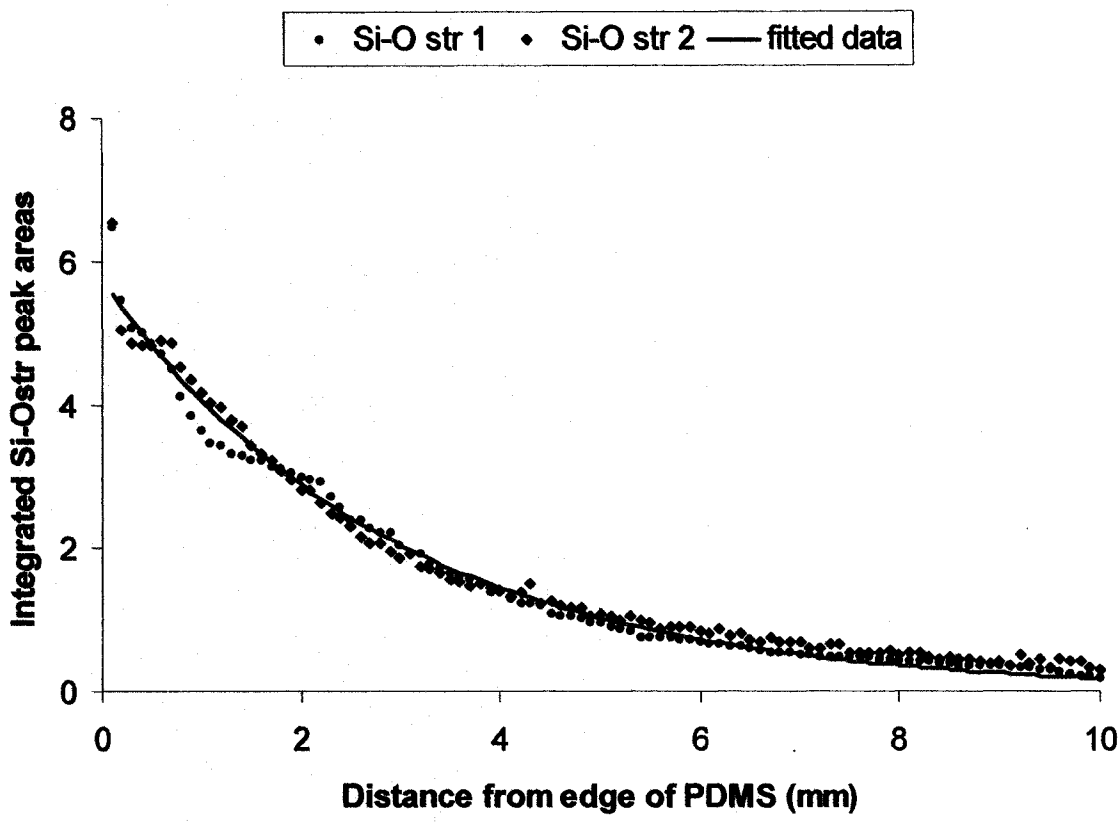

Figure 3.9: The Si-O stretching peak (c in Figure 3.8) was integrated and plotted against the distance away from the edge of PDMS. The spectra were collected from a point at the edge of the PDMS to a point ~10mm away from the PDMS. There was some uncertainty in exactly placing the actual distance of the PDMS from a previously marked line, even with a microscope (the PDMS is transparent to visible light). Spectra were collected from 100x850μm apertures settings using 50 scans.

Figure 3.9 shows the distribution profile obtained in the non-contact areas using FTIR, relating the amount of PDMS transferred onto the gold substrate. Two different sets of experimental data were acquired. The data was fitted with an exponential function: $(y = \exp(-x * a) * b)$, where x is the distance from the edge of the PDMS and **a = 0.3461** and **b = 5.760.** The data is similar to the data obtained using XPS for a similar study (Figure 3.6). The amount of molecules transferred from the PDMS decreases exponentially as the distance away from the PDMS increases. For the peak areas, Figure 3.10 provides a closed-up look on how the area of the Si-O stretching peak was determined.

The mode of transfer of the PDMS molecules seems to be through contact of the native stamp with the substrate. However, the mode of transfer in non-contact areas

could be by gas phase diffusion or movement across the substrate surface or even a combination of the two modes. Figure 3.11 shows the set-up that was used. Two pieces of Au substrates were placed side by side, separated by a 300μm outer diameter wire. One of the Au had contact with PDMS for 2hrs. If the diffusion is across the surface, then it will be safe to assume that no PDMS transfer would occur over the 300μm wire, and therefore, there will be no polymer molecule on the second piece of gold substrate. The result obtained is shown in Figure 3.12.

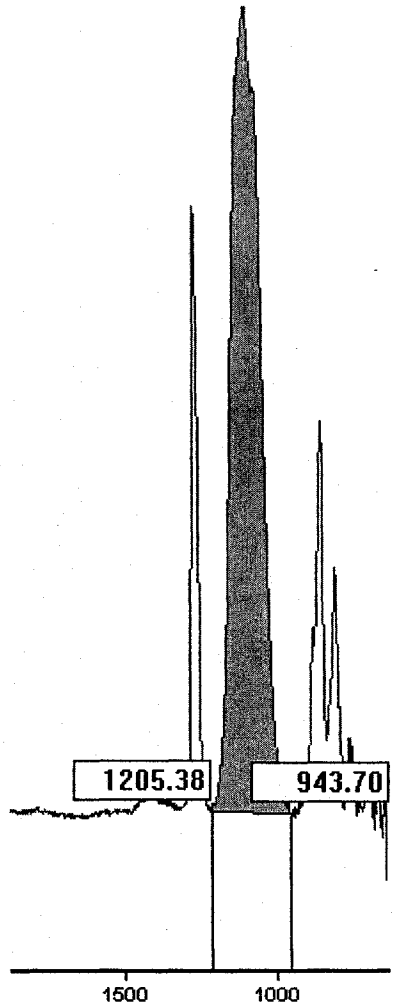

Figure 3.10 is a close up look on how the peak area for the Si-O stretching peaks was determined. Using the instrument software, an integration method was set up by defining a baseline that encompasses only the area under the peak. The peak area was then automatically calculated.

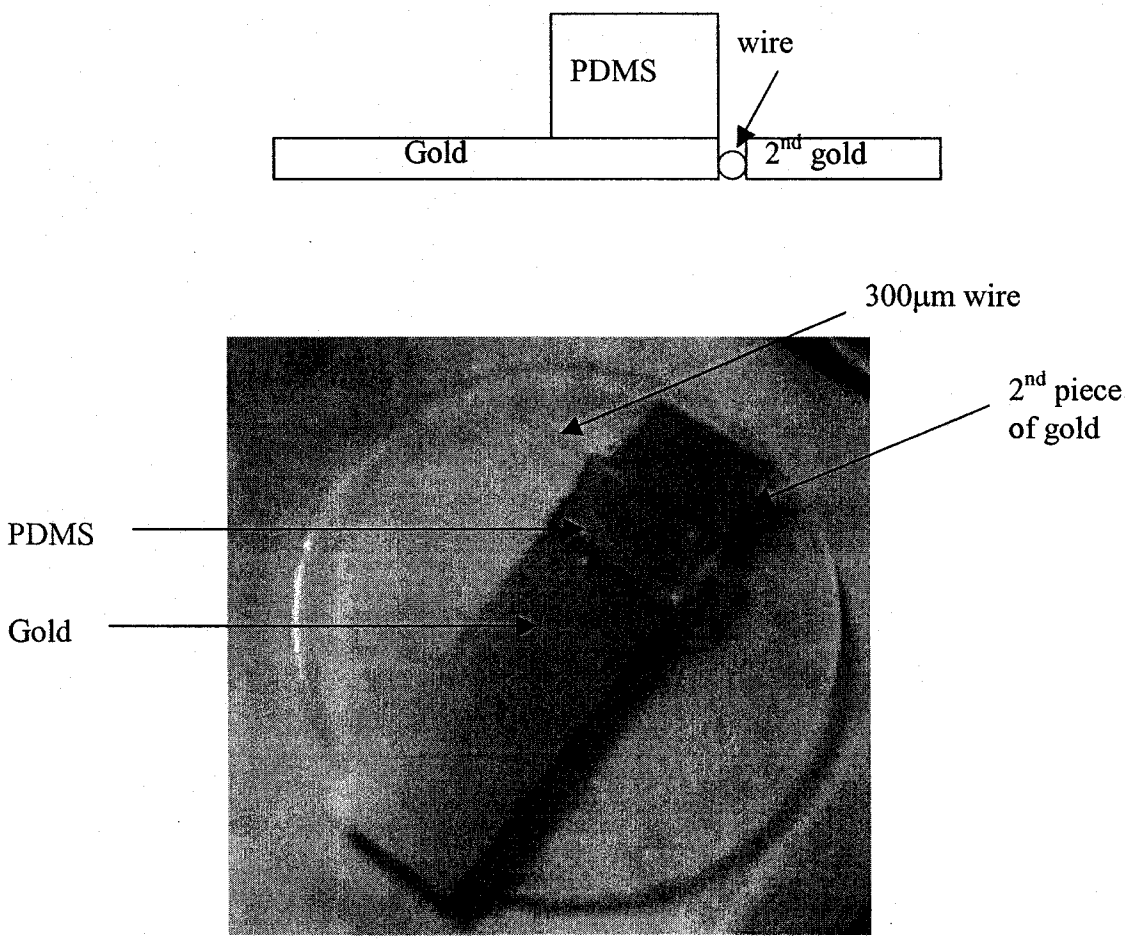

Figure 3.11: Two pieces of gold substrates were separated by a 300μm outer diameter wire. The longer piece of gold had contact with PDMS. The whole set up was covered with a petri-dish to ensure that the only form of transport was by diffusion. The top schematic shows the set-up more clearly.

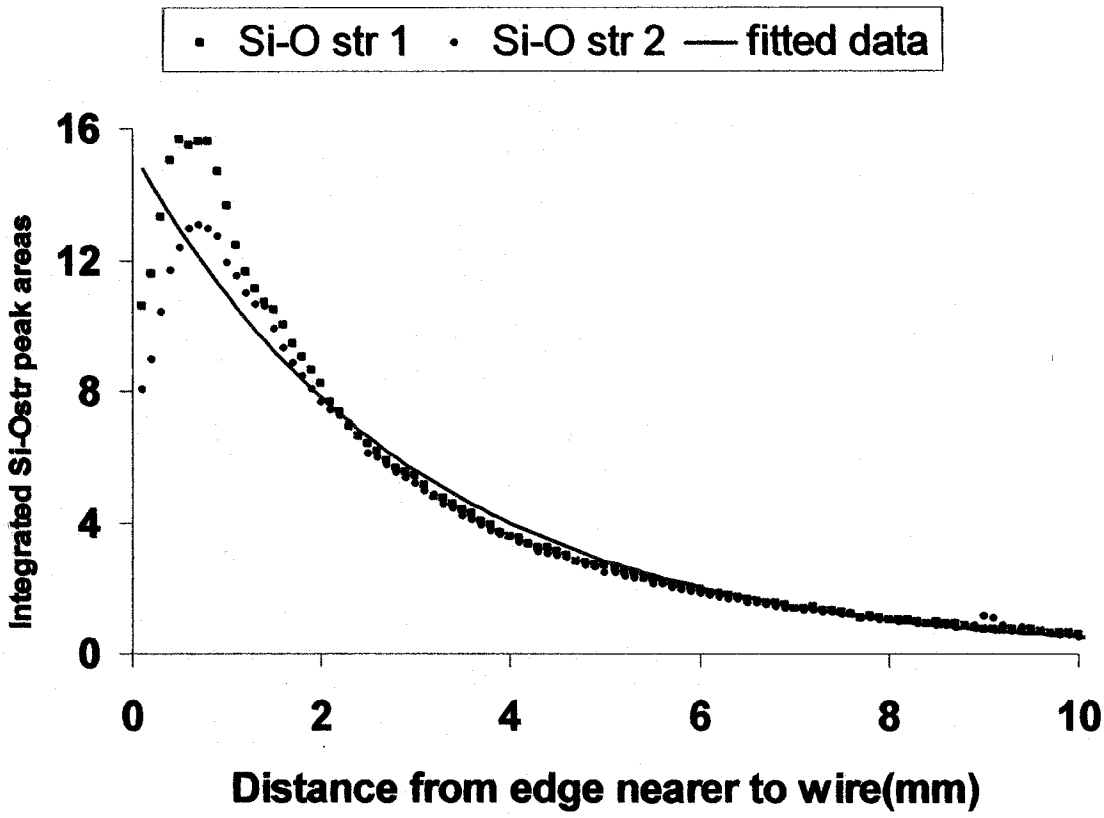

Figure 3.12: Two sets of spectra were collected from 100x200μm areas beginning from the edge closer to the edge of PDMS on the 2nd piece of Au. All spectra were from a single line across the Au surface. 150 scans were used for both background and sample scans. Integrated Si-O stretching peaks were plotted against distance from the wire edge.

Figure 3.12 is a plot showing the integrated peak areas of the Si-O stretching peaks as a function of the distance away from the edge closer to the wire on the second piece of gold. The Figure suggests that the transfer process occurred via gas phase diffusion of the PDMS molecules over the wire. The Petri-dish served to ensure that the transport process is mainly by diffusion of the PDMS molecules. It is also noteworthy that the data showed decreasing amount of molecules transferred along the Au substrate. The decrease in the level of PDMS away from the edge is also consistent with transfer of molecules along the substrate surface. The data was fitted with the equation $(y = \exp(-x * a) * b)$ where x is the distance from the edge of the gold closer to the wire, and **a = 0.336** and **b = 15.27**.

Then we used the grazing angle objective on the microscope to study the diffusion pattern in non-contact areas using 10, 30 and 120mins contact times. A piece

of PDMS was brought into contact for the various contact times and then carefully peeled off. The grazing angle objective was used to map out a straight line through the non-contact areas from where spectra were acquired. The data shown in Figure 3.13 shows a plot of the integrated Si-O stretching peaks against distance from the edge closer to the PDMS contact area. The Figure shows that at these different times, noticeable amounts of the PDMS contaminants were observed in non-contact areas. Looking at the peak areas on the Y-axis, the points directly close to the edge of the PDMS had the most amounts of PDMS molecules transferred. As expected, the longer the contact time, the more uncrosslinked materials are transferred onto the gold substrate.

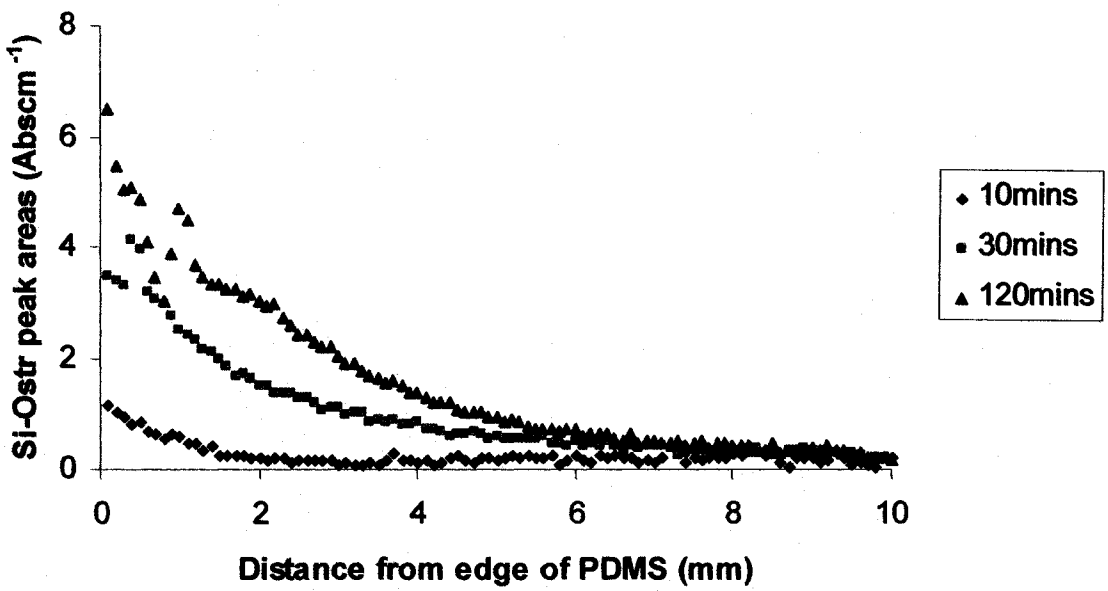

Figure 3.13: PDMS contact times were varied in order to study the distribution of the uncrosslinked molecules in non-contact areas on gold. All the spectra were acquired in the non-contact areas on the Au substrates using 50 scans with an aperture size of 100x850μm. The Si-O stretching peaks were integrated and plotted against the distance away from the edge of PDMS contact.

3.3.4 Contamination in microfluidic channels

The Si master used had a series of microfluidic channels and wells. The well area was $1mm^2$. When a PDMS stamp cured using this master was brought into contact with the Au substrate, the wells do not make contact with the surface. An image of the area analyzed on the substrate after contact is shown in Figure 3.14. The circled areas on the image are interference patterns that suggest that many PDMS molecules had been transferred onto the Au substrate. This suggestion is even more evidenced by the fact the interference patterns are visible to the naked eyes.

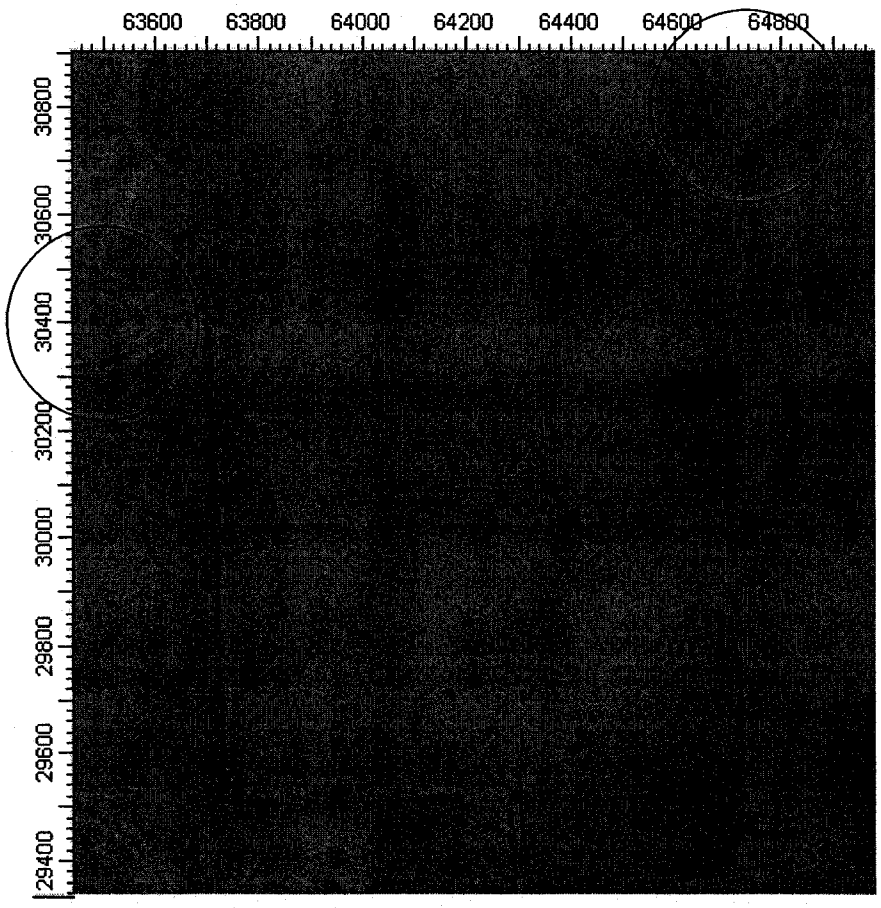

Figure 3.14: An optical image of a similar well area used for the experiment. The well is $1mm^2$ with a channel exiting at the lower end. Twenty-five spots were taken from either side of the well. One hundred spots were analyzed within the well. All the spots lie on a single line across the well. Each of these apertures settings was $100x200\mu m$ in steps of $10\mu m$. 150 scans were used at $2cm^{-1}$ resolution.

The data shown in Figure 3.15A is a plot of the distribution of PDMS molecules within the microfluidic well. The first and last twenty-five data points were obtained from the contact areas outside the well while the middle one hundred data points were from within the well. The result suggests that the likely mechanism of transport of these molecules in non-contact areas is by vapor phase diffusion followed by the subsequent transfer along the substrate surface. The Figure also suggests that vapor diffusion from the "ceiling" is negligible as evidenced by the very small signal obtained from areas around the middle of the well (Figure 3.15B). The areas ~25μm on either side of the well (contact areas) showed relatively large amount of PDMS molecules, but quickly decreased down the well. Inside the well, the first 100μm or so on each side, showed significant contamination compared to the remaining parts. This transfer of uncrosslinked PDMS onto the substrate within the well would result in a hydrophobic surface, which depending on intended application, could be quite detrimental.

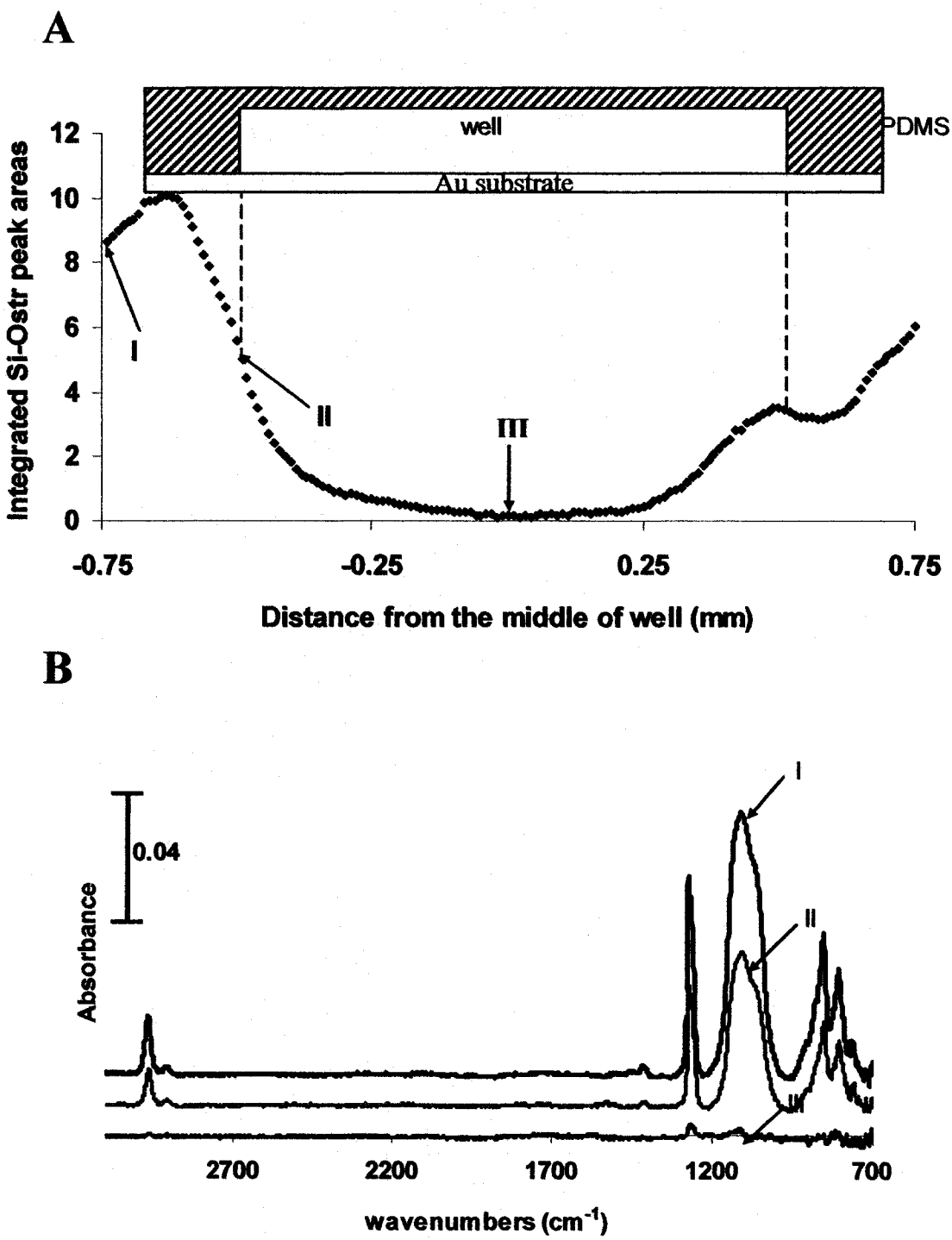

Figure 3.15A shows how the transferred PDMS molecules are distributed within and outside the well, with a schematic of the experimental set-up. Si-O stretching peaks were integrated and plotted against the distance from the middle of the well. A schematic of the well is overlaid on the plot to indicate the data obtained from within the well. Figure 3.15b shows the offset spectra for the indicated data points in 3.15A (I) is a spectrum from outside the well in a contact area; (II) is the first spectrum acquired within the well, and (III) is the spectrum obtained from the middle point within the well.

In order to better comprehend the contribution of both the sides and the top "ceiling" on the distribution of PDMS within the well, two experiments were carried out. In the first experiment to study the contribution from the sides, a hole was made within a piece of flat PDMS by curing the PDMS around a $1cm^2$ cuvette. The PDMS was then brought into conformal contact with a gold substrate for 2hrs. Figure 3:16 is a plot of the integrated Si-O stretching peak areas as a function of the distance from one edge of the hole to the other. The plot shows a similar pattern of transfer of PDMS molecules within a microfluidic well (Figure 3:15A), thereby suggesting the transfer is by gas phase diffusion. However, it also shows that there is significant contribution from the sides, which in this case represents the sides within the microfluidic well.

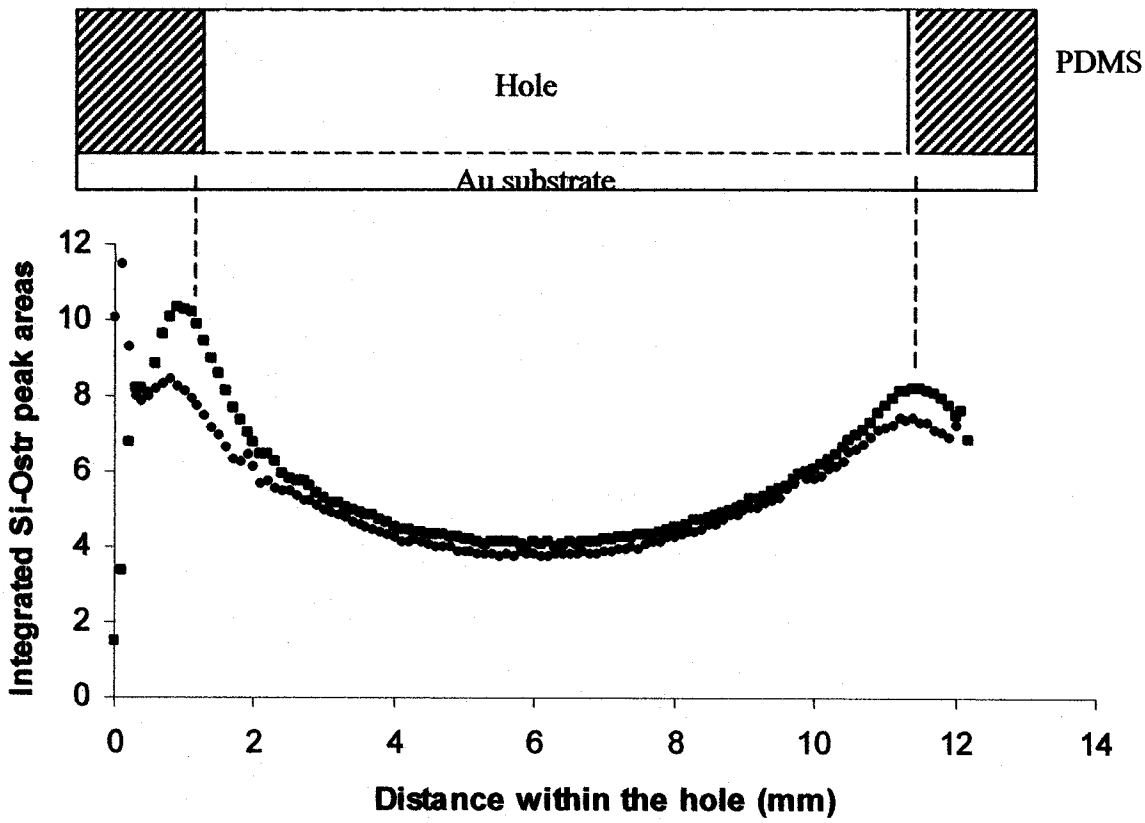

Figure 3:16 Si-O stretching peak areas of the PDMS within the hole. The contact time was 2hrs. Two data sets were acquired. Fifty scans were used for both background and sample spectra with an aperture size of 100x850μm. A schematic of the PDMS hole is overlaid on 3.16 for clarity

In the second experiment to study the contribution from the top, a piece of aluminum foil (13μm thick) with a 7 x 7mm hole was placed on top of a piece of native

PDMS. A gold substrate was then placed on top of the whole assembly such that there was no contact between the PDMS and the gold, for 2hrs. Only vapors from the PDMS could reach the gold through the 7 x 7mm hole made in the foil. Figure 3:17 is a plot of the integrated Si-O stretching peak areas against the distance from one side of the hole on the gold to the other side. The Figure does not show any particular pattern, but it is quite clear that PDMS molecules were transferred by gas phase onto the gold substrate.

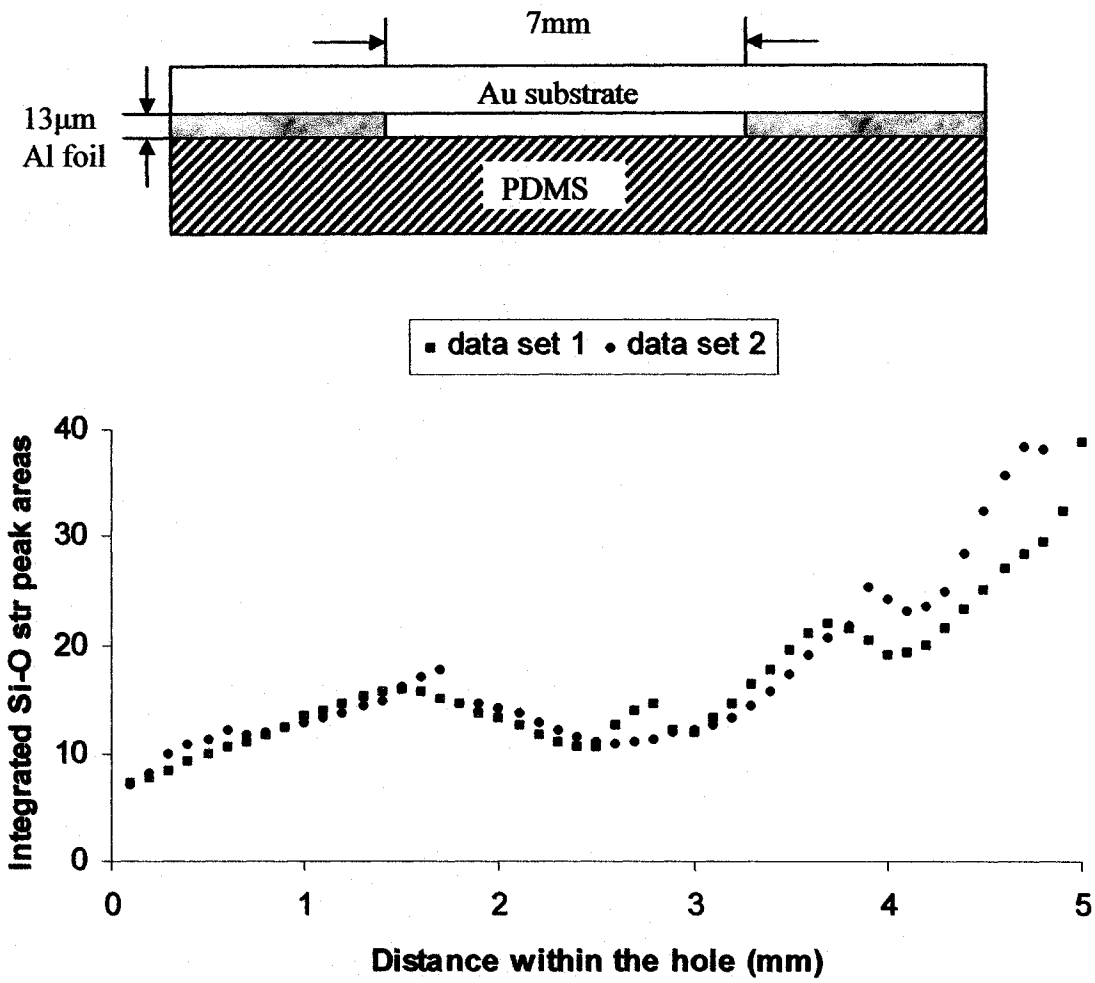

Figure 3:17 Plot of integrated Si-O stretching peak areas of the PDMS on gold through the square hole in the foil against a 5mm distance around the middle of the hole. Two data sets were acquired. The contact time was 2hrs. Fifty scans were used for both background and sample spectra with an aperture size of 100x850μm. A schematic of the experimental set-up is shown for clarity.

3.3.5: Studies on the effects of different cleaning methods on PDMS

The cold extraction and cold extraction with systematic deswelling of PDMS methods bear very close similarities with those found in literature [6, 22], with only minor variations. In the cold extraction method found in literature [6], the drying of the PDMS preceded the sonication step, which is the reverse in the procedure used in this study. In the systematic drying method, pentane was used in the literature [22] instead of hexane, and the PDMS was oven-dried for two days instead of one as was used in this study. The extracted PDMS were then brought into conformal contact with gold substrate for 2hrs. Figure 3.18 is the plot obtained when bringing both the native and extracted PDMS into contact with a gold substrate. The integrated C-H stretching peak areas were plotted against the distance from the edge closer to the PDMS contact area. The plot shows that for all three methods, after one extraction step, most if not all, of the uncrosslinked molecules had been extracted. While all the methods give satisfactory results, it is worthy of note that the hot extraction method is much faster in terms of procedure.

Whitesides *et al* [22] used cohesive energy density (cal/cm^3) to calculate solubility (or degree of swelling in the case of crosslinked polymers). Using the data from the degree of swelling of PDMS the authors were able to classify organic solvents into four categories: low, moderate, high and extreme solubility solvents. Those with high solubility include aliphatic and aromatic hydrocarbons (pentanes, hexanes, benzene, and toluene), halogenated compounds and ethers. These are able to swell the PDMS and in the process extract the uncrosslinked molecules.

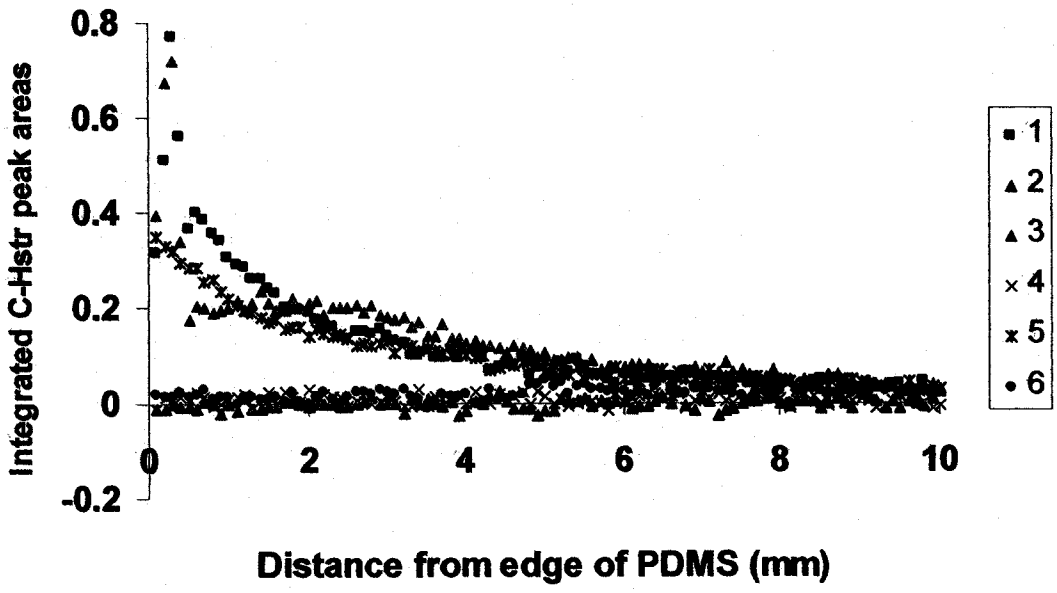

Figure 3.18: Three different native PDMS stamps were brought into contact with Au substrates. The stamps were subsequently extracted using different extraction methods. The extracted PDMS were then brought into contact again with Au substrates. 1) before hot extraction of native PDMS, 2) after hot extraction, 3) before cold extraction with systematic deswelling, 4) after cold extraction with systematic deswelling, 5) cold extraction, 6) after cold extraction

3.4: Conclusions

These studies were able to demonstrate the inhomogeneity associated with the transfer of PDMS molecules in contact areas while also describing the distribution profile of these molecules in non-contact areas using surface sensitive techniques such as XPS and FTIR. Even short contact times resulted in transfer of PDMS. The mode of transfer seems to be different for the contact and non-contact areas. In contact areas, transfer is across the contact surface while the molecules diffuse in the gas phase onto non-contact areas and subsequently transferred across the substrate surface. This mode of transfer is further supported by studying the distribution profile in microfluidic wells (non-contact area when brought into contact with Au substrate).

Extraction of these uncrosslinked molecules from the bulk PDMS using high solubility solvents such as hexane (either cold or hot extractions) proved very useful in reducing the level of contamination from the bulk PDMS onto gold substrates.

3.5 References

1 A. Kumar and G. M. Whitesides, *Appl. Phys. Lett.* **1993**, *63*, 2002

2 J. L.Tan, J. Tien and C. S. Chen, *Langmuir* **2002,** *18,* 519-523

3 E. Delamarche, A. Bernard, H. Schmid, A. Bietsch, B. Michel, and H. Biebuyck, *J. Am. Chem. Soc.* **1998**, *120,* 500

4 C. S. Effenhauser, G. J. M. Bruin, A. Paulus, and M. Ehrat, *Anal. Chem.* **1997,** *69*, 3451

5 I. Bohm, A. Lampert, M. Buck, F. Eisert and M. Grunze, *Appl. Surf. Sci,* **1999,** *141,* 242

6 D. J. Graham, D. D. Price and B. D. Ratner *Langmuir* **2002,** *18,* 1526

7 K. Glassmaster, J. Gold, A. Andersson, D.S. Sutherland, and B. Kasemo *Langmuir*, **2003**, *19*, 5475

8 K. Pandian and G. A. Nirmala, *J Solid State Electrochem* **2003,** *7,* 298

9 M. L. Tingey, S. Wilyana, E. J. Snodgrass, and N. L. Abbott *Langmuir* **2004,** *20,* 6823

10 K. Felmet and Y.-L. Loo, *Appl. Phys. Lett.*, **2004**, *85*, 3317

11 J. Rickert, T. Weiss, and W. Gtpel *Sensors and Actuators B* **1996,** *31,* 45-50

12. C. J. Powell, A. Jablonski, W. S. M. Werner and W. Smekal, *Appl. Surf. Sci* **2005,** *239,* 470

13 W. Prissanaroon, N. Brack, P.J. Pigram, P. Hale, P. Kappen and J. Liesegang *Thin Solid Films*, **2005**, *477,* 131

14 Z. Yang, A.M. Belu, A. Liebmann-Vinson, H. Sugg, and A. Chilkoti, *Langmuir* **2000,**

16, 7482

15 Y. Zhou, R. Valiokas, and B. Liedberg *Langmuir* **2004,** *20,* 6206

16 Bjork, P., Herland, A., Scheblykin, I.G., and Inganas, O. *Nanoletters*, **2005**, *5*, 1948-1953

17 X. Wang, M. Ostblom, T. Johansson and O. Inganas *Thin Solid Films,* **2004**, *449,* 125

18 X. Wang, K. Tvingstedt, and O. Inganas *Nanotech.* **2005**, *16*, 437–443

19 A. F. Runge, and S. S. Saavedra *Langmuir,* **2003,** *19,* 9418-9424

20 F. Bensebaa, P. L'Ecuyer, K. Faid, T.J. Tague, R.S. Jackson *Applied Surface Science,* **2005,** *243,* 238–244

21 S. M. Hunt and G. A. George *Polymer Int.,* **2000,** *49* 634

22 J. N. Lee, C. Park, and G. M. whitesides *Anal. Chem.* **2003**, *75*, 6544

23 S. C. Yoon, B. D. Ratner, B. Ivan and J. P. Kennedy *Macromolecules,* **1994**, *27*, 1549

24 P. A. Donald and J. C. Stephen *Surface & Coatings Tech.* **2004**, *187*, 199

25 V. H. Rita, V. V. Luc, A. Annemie and A. Freddy *Anal. Chim. Acta* **2003**, *500,* 259

26 M. J. Owen, and P. J. Smith, *J. Adhes. Sci.Technol.* **1994**, *8*, 1063

27 K. Efimenko, W. E. Wallace, and J. Genzer *J. of Col. and Interface Science,* **2002,** *254*, 306

28 E. Pavlovic, A. Quist, L. Nyholm, A. Pallin, U. Gelius, and S. Oscarsson, *Langmuir* **2003,** *19,* 10267-10270

29 B. A. Langowski and K. E. Uhrich, *Langmuir* **2005**, *21,* 6366

30 S. W. Howell, H. D. Inerowicz, F. E. Regnier, and R. Reifenberger, *Langmuir,* **2003**, *19,* 436

31 H. Hillborg and U.W. Gedde *Polymer* **1998,** *39,* 1991

32 H. Hillborg, M. Sandelin and U.W. Gedde *Polymer* **2001**, *42,* 7349

CHAPTER 4

GENERAL CONCLUSIONS.

4.1 Conclusions

Polydimethylsiloxane, or PDMS, is a very important elastomer in every one of its numerous applications [1-3]. It has been demonstrated in this work and in several other papers [4-6] that residues from PDMS can diffuse to the substrate, and in the process modify the substrate's surface properties such as hydrophobicity and wetting properties. One of the reported cases has harnessed such substrate modification into positive use [7], however most have shown its detrimental effects [8, 9].

Analysis of the PDMS extract using MALDI and ESI data showed that the contaminant molecules most likely came from uncrosslinked, elastomer base molecules as opposed to the curing agent. A 10:1 elastomer base/curing agent ratio might just make the base materials to be in excess. Semi-quantitative data obtained from MALDI showed that the extracted PDMS molecules were significantly more than in the first extract than the other extracts. That also confirmed the fact that hexane is a very good solvent that can be used to clean the PDMS, regardless of the method used in doing so.

Infrared and x-ray spectroscopy (FTIR and XPS) [10, 11] are two sensitive surface characterization methods used in this study. Both confirmed the presence of PDMS molecules on the substrate that has been in contact with the native, unextracted elastomer [12]. However, the presence of PDMS molecules in non-contact areas has not been studied before.

Both XPS and FTIR showed that from the regions directly away from PDMS contact, there is a build-up of PDMS molecules, the amount of which decreases as the distance from the PDMS increases. This distance dependence concentration gradient is identical whether the study was done with microfluidic channels or during microcontact printing. The same pattern was also observed when a gold substrate having the native PDMS contact was separated from another gold substrate by a 300μm wire, in a study aimed at understanding the mode of transport of these PDMS molecules on a substrate surface into regions of non-contact. This observation led us to believe that it was mostly

by gas phase transport as opposed to by surface transport in areas where the PDMS had contact with a substrate.

There is therefore no doubt that if the unextracted, native PDMS had been used in the process of nanodevice fabrication, it might have affected the entire process. On the strength of the few data presented here and what has been reported elsewhere [13], there is a strong indication that the fabrication of a polyaniline single molecule using electrochemical dip-pen nanolithography can be achieved on a substrate that has been modified with a mixed monolayer of 4-aminothiophenol and octadecanethiol. It has been shown that nanoislands of 4-ATP can be used to selectively oxidize aniline monomer in a sea of ODT using conventional cyclic voltammetry [14].

The AFM nanolithography abilities have also been demonstrated, with the added advantage of the program that can help direct the tip movement.

4.2 Future prospects

As to the future, I think the next phase is to design intelligent experiments in order to optimize the different parameters that certainly would have an effect on polymerization process such as humidity, temperature, tip bias and scan rate and the different concentrations of the monomer, dopant ion and mixed monolayer fractions. This will eventually lead to actually carrying out the polymerization using all the optimized parameters.

4.3 References

1 J. F. Hall *IEEE Transactions on Power Delivery*, **1993**. *8*, 376

2 M. M. Ngundi, L. C. Shriver-Lake, M. H. Moore, M. L. Lassman, F. S. Ligler, and C. R. Taitt, *Anal. Chem.* **2005**, *77*, 148

3 J. L. Tan, J. Tien, and C. S. Chen, *Langmuir* **2002**, *18*, 519-523

4 Z. Yang, A. M. Belu, A., Liebmann-Vinson, H. Sugg, and A. Chilkoti *Langmuir* **2000**, *16*, 7482

5 Y. Zhou, R. Valiokas, and B. Liedberg *Langmuir* **2004**, *20*, 6206

6 J. N. Lee, C. Park, and G. M. Whitesides *Anal. Chem.* **2003**, *75*, 6544

7 P. Bjork, A. Herland, I. G. Scheblykin, and O. Inganas *Nanoletters*, **2005**, *5*, 1950

8 K. Felmet and Y.-L. Loo, *Appl. Phys. Lett.*, **2004**. *85*, 3317

9 X. Wang, M. Ostblom, T. Johansson, O. Inganas *Thin Solid Films,* **2004**, *449* 125

10 K. Efimenko, W. E. Wallace, and J. Genzer *J. Col. and Interface, Science* **2002** *254*, 306

11 P. A. Donald, J. C. Stephen *Surface & Coatings Tech.* **2004**, *187*, 199

12 K. Glassmaster, J. Gold, A. Andersson, D. S. Sutherland, and B. Kasemo *Langmuir*, **2003**, *19*, 5475

13 S. Jegadesan, R.C. Advincula and S. Valiyaveettil *Adv. Mater.* **2005**, *17*, 1282-1285

14 W. A. Hayes and C. Shannon *Langmuir* **1998**, *14*, 1099-1102